

Unveiling the global urban virome through wastewater metagenomics

Received: 10 March 2025

Accepted: 8 October 2025

Published online: 28 November 2025

 Check for updates

Nathalie Worp ¹, David F. Nieuwenhuijse ¹, Ray W. Izquierdo-Lara ¹,
Claudia M. E. Schapendonk¹, Christian Brinch ², Emilie Egholm Bruun Jensen ²,
Patrick Munk ², Rene S. Hendriksen³, Global Sewage Surveillance Consortium*,
Frank Aarestrup ², Bas B. Oude Munnink ¹, Marion P. G. Koopmans ^{1,178} &
Miranda de Graaf ^{1,178} 

Understanding global viral dynamics is critical for public health. Traditional surveillance focuses on individual pathogens and symptomatic cases, which may miss asymptomatic infections or newly emerging viruses, delaying detection and response. Wastewater-based epidemiology has been used to track pathogens through targeted molecular assays, but its reliance on pre-defined targets limits detection of the full viral spectrum. Here, we analyse longitudinal wastewater samples from 62 cities across six continents (2017–2019) using metagenomics and capture-based sequencing with probes targeting viruses associated with gastrointestinal disease. We detect over 2500 viral species spanning 122 families, many with human, animal, or plant health relevance. The bacteriophage family *Microviridae* and plant virus family *Virgaviridae* dominate the metagenomic dataset, while *Astroviridae* and *Picornaviridae* prevail in the capture-based sequence dataset. Virus distributions are broadly similar across continents at the family and genus levels, yet distinct city-level fingerprints reveal geographical and temporal variation, enabling spatiotemporal surveillance of viruses such as astroviruses and enteroviruses. Global wastewater-based epidemiology enables early detection of emerging viruses, including Echovirus 30 in Europe and *Tomato brown rugose fruit virus*. These findings highlight the potential of wastewater sequencing for the early detection of emerging viruses and population-wide virome monitoring across diverse hosts.

In recent decades, the frequency and scale of infectious disease outbreaks have increased, particularly those emerging after spillover of animal viruses¹. The emergence and spread of these diseases have been driven by a range of interconnected factors, including urbanization², the development of megacities³, deforestation^{4,5}, growing food demands⁶, and increasing global connectivity. Migration from rural to

urban areas has contributed to population growth in cities, resulting in increased close-contact interactions that facilitate disease transmission³. By 2017, 55% of the world's population lived in urban areas⁷, making these high-density cities critical hubs for the spread of infectious diseases, and therefore strategic sites for monitoring and responding to both novel and established public health threats.

¹Department of Viroscience, Erasmus University Medical Center, Rotterdam, the Netherlands. ²Research Group for Genomic Epidemiology, Technical University of Denmark, Kgs, Lyngby, Denmark. ³Research Group for Global Capacity Building, National Food Institute, Technical University of Denmark, Kgs, Lyngby, Denmark. ¹⁷⁸These authors contributed equally: Marion P. G. Koopmans, Miranda de Graaf. *A list of authors and their affiliations appears at the end of the paper. ✉e-mail: m.degraaf@erasmusmc.nl

Current infectious disease surveillance primarily relies on the identification and reporting of symptomatic cases³, which has limitations, particularly for viruses that frequently cause asymptomatic or mild infections, or diseases that are not reportable. As a result, novel infectious diseases caused by emerging viruses or variants of known viruses can evade detection, spreading silently before being recognized. This phenomenon was exemplified by the introduction of Zika virus in South America⁹ and the early undetected spread of SARS-CoV-2 into Europe^{10,11} and the USA¹². To better understand the prevalence and spread of viral infections, alternative surveillance strategies beyond symptom-based reporting are needed to capture the full spectrum of viral transmission dynamics and enhance early detection and response to emerging infectious disease threats.

Wastewater-based epidemiology (WBE) involves the detection and monitoring of chemicals, drugs and substances^{13,14}, genes¹⁵, pathogens¹⁶ and vectors¹⁷ within wastewater to assess community health or disease risk. Recent detections of poliovirus in wastewater from major urban cities like New York¹⁸, London¹⁹, and poliovirus essential facilities²⁰ highlight the potential of WBE in identifying circulation hotspots and guiding targeted interventions, such as enhancing surveillance and launching of vaccine campaigns¹⁷. During the COVID-19 pandemic, quantitative reverse transcription PCR-based methods were used to assess the viral load in wastewater, with viral concentrations following the number of positive cases at the community level and providing insights into infection dynamics over time^{19,20}. Amplicon-based sequencing was used in parallel to identify circulating viral variants, enhancing early detection capabilities in wastewater if used in combination with pathogen specific bioinformatic pipelines^{21,22}. Utilizing targeted molecular methods has extended WBE to track other pathogenic viruses like influenza²³, respiratory syncytial virus²³, mpox²⁴, arboviruses²⁵, and non-polio enteroviruses (EV) such as EV-D68²⁶.

Among viruses shed into wastewater, enteric viruses pose a significant public health threat. Enteric viruses mainly transmit through the faecal-oral route, cause a wide range of gastrointestinal diseases and are potential sources of community-wide outbreaks²⁷. Detection is complicated by their extensive diversity, nonspecific clinical symptoms that hamper diagnosis, high rate of secondary transmission which may mask initial introductions, and gaps in surveillance systems. As the number of viral targets of interest grows, the question arises whether surveillance efforts focused on individual pathogens can be combined in a more

comprehensive approach. In this context, metagenomic sequencing can be a promising technique that can address this need²⁸. A significant advantage of metagenomic sequencing is its ability to simultaneously detect and characterize multiple viral agents present within a single (wastewater) sample including non-target (novel) viruses^{29,30}.

In this study, we explore the potential of metagenomic sequencing and analysis as a tool for population level monitoring of virus circulation across hosts in high-density urban areas. We sequenced and characterized the wastewater virome of 62 major cities worldwide using both a shotgun viral metagenomic and a capture based sequencing method targeting enteric viruses, to compare viromes and viral dynamics across the world. Our findings reveal city-specific virome fingerprints and show that wastewater metagenomics enables early detection of emerging viruses and can inform broader epidemic surveillance.

Results

Virome data overview

To investigate the worldwide urban wastewater virome, wastewater samples were collected from 62 cities across 47 countries on 6 continents (Fig. 1)³¹. For all cities, samples were acquired biannually in June and November over a 2 year period spanning 2017–2019 (biannual samples). Additionally, to investigate temporal changes, monthly samples were obtained from eight cities in different countries in six different continents during the same period. Wastewater samples were analysed using both shotgun viral metagenomic sequencing to determine the viral metagenome and sequencing following capture using a custom probe set (GastroCap, Supplementary Fig. 1), designed to enrich for enteric virus sequences. The median number of reads generated after sequencing was 9.8×10^5 (IQR: 6.9×10^5 – 1.26×10^6) per sample for the metagenomic sequence dataset and 7.4×10^5 (IQR: 4.6×10^5 – 1.17×10^6) for the capture sequence dataset (Supplementary Fig. 2). The median percentage of reads per sample that could be annotated as viral was 11% (IQR: 6.5–15.3%) for the metagenomic sequence dataset and 26% (IQR: 11.8–46.9%) for the capture sequence dataset. The remaining reads were annotated as bacterial, human, other eukaryotic, or unclassified (i.e., without any annotation) (Supplementary Fig. 2). Principal component analysis (PCA) of centred log-ratio (CLR) transformed read count data at the superkingdom level revealed distinct clustering between the two datasets and confirmed the enrichment of viral reads using GastroCap (Supplementary Fig. 3).

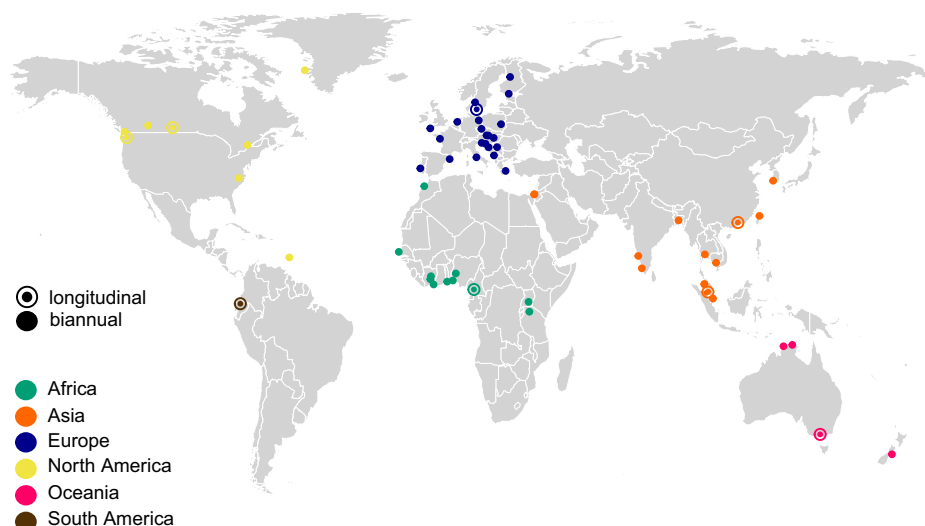


Fig. 1 | Overview of the 62 wastewater collection sites. Cities are coloured by continent and categorized by sampling strategy: colour-filled dots represent cities with biannual sampling, while outlined dots represent cities with longitudinal sampling.

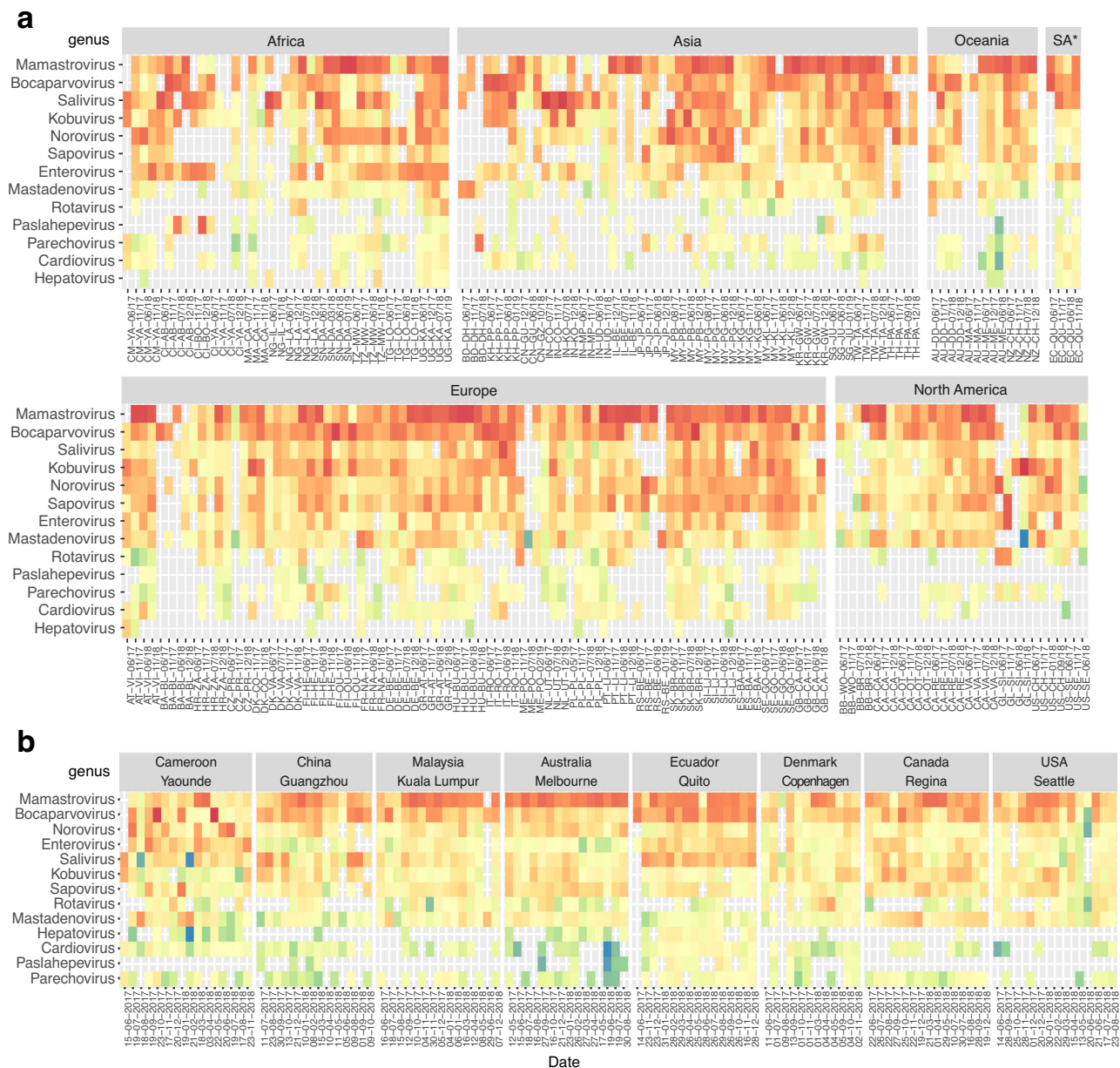


Fig. 3 | Pathogenic enteric viruses were widespread and showed distinct spatiotemporal patterns in urban wastewater. Reads per million viral reads (normalized by genome length) per genus are given for the biannual (a) and longitudinal (b) GastroCap sample set. The heatmap is ordered by reads per million

viral reads (normalized by genome length) and categorized by continent (a) and city (b). The colour gradient represents log-transformed relative abundance of reads. SA South America.

Composition of the Global Urban Wastewater Virome

To establish a baseline understanding of the urban wastewater virome, we first examined the diversity of viruses at the family level. Overall, viral reads were mapped to a total of 122 families, 1367 genera and 2546 species (Fig. 2). These findings highlight the broad diversity of viruses associated with vertebrates, plants, microbes, and other life forms within urban environments. A large fraction of the metagenomic virome consisted of bacteriophages and plant viruses (Fig. 2). Viral families linked to human disease, such as *Astroviridae*, *Parvoviridae*, and *Picornaviridae*, were frequently detected in high abundances. In contrast, other important human-associated families, including *Adenoviridae*, *Caliciviridae*, *Hepeviridae*, and *Sedoreoviridae*, were also detected but less frequently.

Of the eight viral families targeted by GastroCap (*Adenoviridae*, *Astroviridae*, *Caliciviridae*, *Hepeviridae*, *Parvoviridae*, *Picornaviridae*,

Spinareoviridae and *Sedoreoviridae*) which include 72 genera and 1038 species, a total of 72 genera and 165 species were identified (Fig. 2). GastroCap-based sequencing resulted in a substantial increase in both the total and relative number of reads for the targeted viral families. The median fold increase per sample, based on relative abundance in reads per million (rpm), was as follows: *Adenoviridae* (545-fold), *Astroviridae* (470-fold), *Caliciviridae* (5094-fold), *Hepeviridae* (22-fold), *Parvoviridae* (2-fold), *Picornaviridae* (132-fold), *Sedoreoviridae* (193-fold) and *Spinareoviridae* (21-fold). Viral genera associated with human gastrointestinal disease, including those commonly targeted by surveillance, such as *Mamastrovirus*, *Bocaparvovirus*, *Salivirus*, *Kobuvirus*, *Norovirus*, *Sapovirus*, *Enterovirus*, *Mastadenovirus*, *Rotavirus*, *Paslahepevirus*, *Parechovirus*, *Cardiovirus* were detected across all continents. However, while *Mamastrovirus* was highly abundant in most samples across all

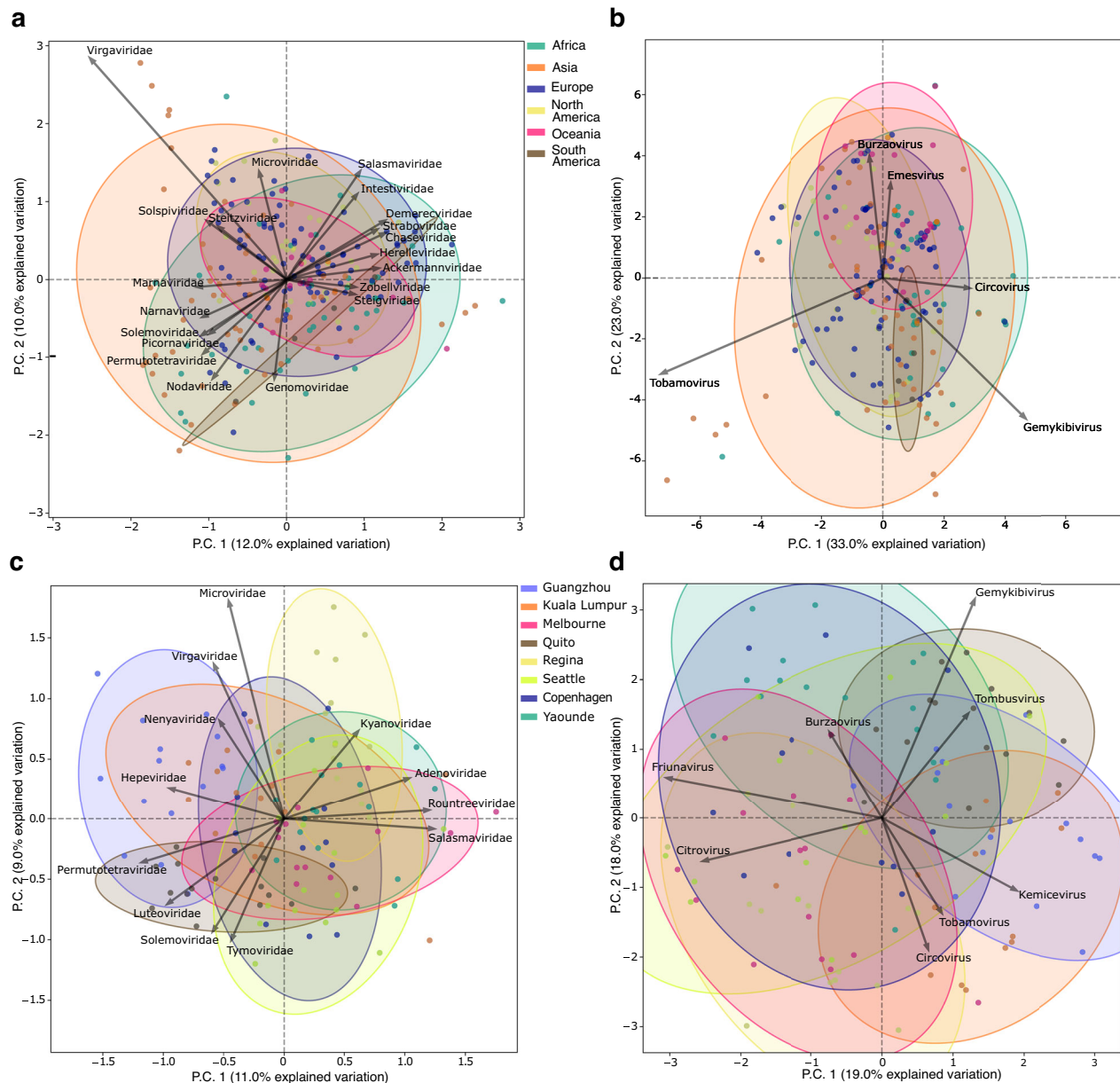


Fig. 4 | PCA clustering of the urban wastewater virome compositions from 62 cities based on the shotgun metagenomic sequence dataset reveals city-level differences without clear continental clustering. The virome compositions of the biannual samples (a, b) coloured by continent and longitudinal samples (c, d) coloured by city at the family (a, c) and genus (b, d) levels. Principal components

were derived from genome size adjusted read counts subjected to a CLR transformation. Arrows represent viral families or genera, with their direction showing their contribution to the principal components and their length indicating the strength of their contribution to the variance in virome composition.

continents (Fig. 3a), *Enterovirus* was mainly detected at high levels in samples from Africa, a few cities in Europe (Belgrade, Bratislava), North America (Sisimiut, Chapel Hill), and South America (Quito) (Fig. 3b). Conversely, *Paslahepevirus*, to which Hepatitis E belongs, was more prevalent in Europe than in other regions. The longitudinal samples further revealed distinct spatial and temporal patterns in the prevalence of certain gastrointestinal viruses. For example, in Regina (Canada), *Enterovirus* levels showed a relative increase during summer months, whereas *Mastadenovirus* abundance was higher in the winter months.

Principal Component Analysis revealed that cities differ in virome composition

To identify broader patterns and potential geographical signatures in virome composition, we applied principal component analysis (PCA)

on both the metagenomic and GastroCap sequence datasets. The metagenomic sequence data revealed no clear clustering patterns across continents at either the family or genus level, suggesting that the viral community structures were broadly similar worldwide (Fig. 4a, b). The limited variance between locations was primarily driven by the genera *Tobamovirus* (a group of plant viruses within the *Virgaviridae* family) and *Gemykibivirus* (associated with multiple hosts, including plants, insects, mammals, and occasional human samples³²), both of which were more prevalent in samples from Asia. However, when comparing the virome composition by city, more pronounced differences were observed in both biannual and longitudinal samples (Supplementary Fig. S4 and Fig. 4c, d). This pattern was consistent when performing the PCA separately for DNA and RNA viruses (Supplementary Figs. 6 and 7), supporting the robustness of these findings across viral genome types.

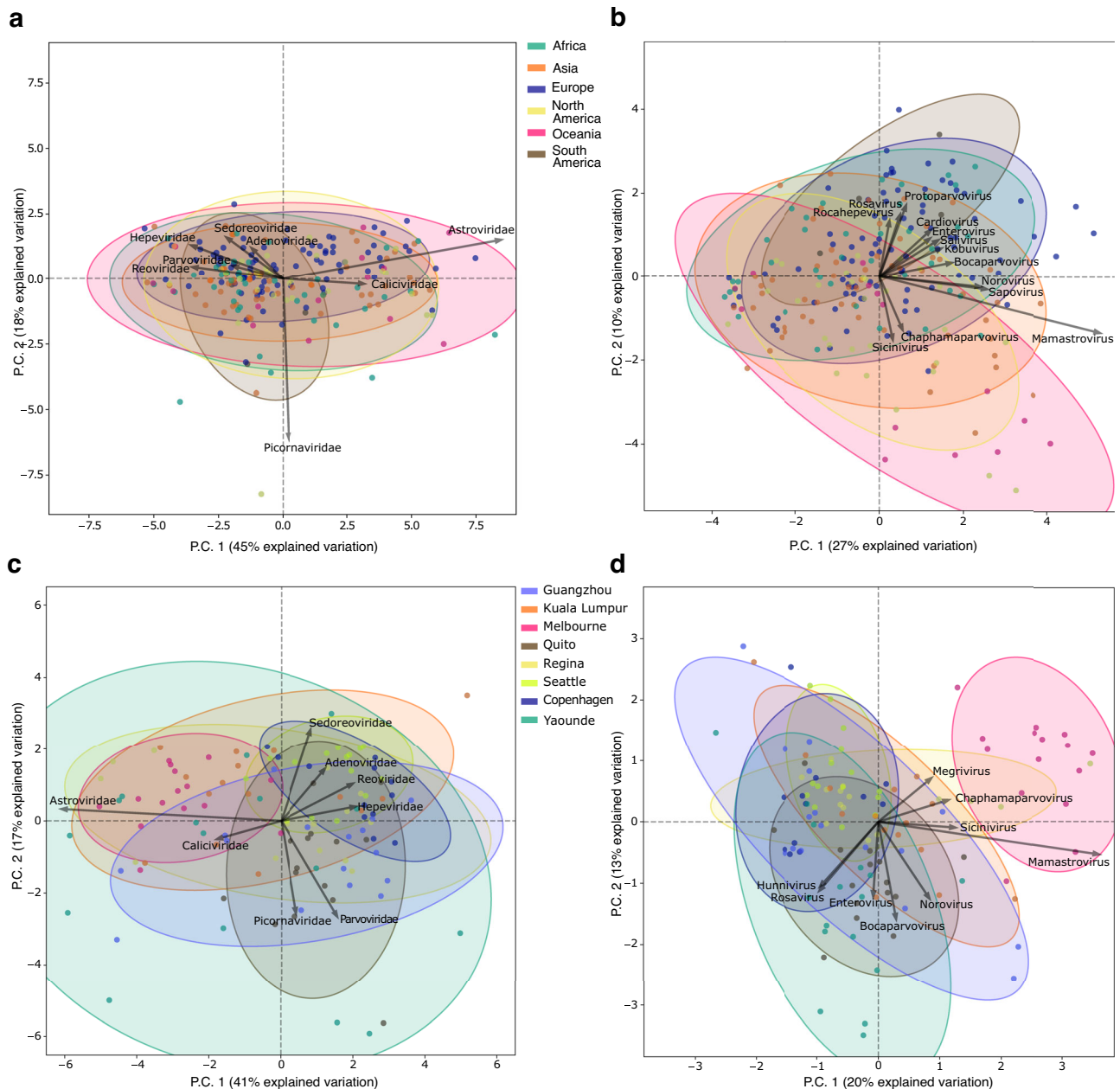


Fig. 5 | PCA clustering of the urban wastewater virome compositions from 62 cities based on the GastroCap sequence dataset highlight city-level clustering, primarily driven by *Mamastrovirus*. The virome compositions of the biannual samples (a, b) coloured by continent and longitudinal (c, d) samples coloured by city at the family (a, c) and genus (b, d) levels. Principal components were derived

from genome size adjusted read counts subjected to a CLR transformation. Arrows represent viral families or genera, with their direction showing their contribution to the principal components and their length indicating the strength of their contribution to the variance in virome composition.

Focusing on the enteric virus families in the GastroCap sequence dataset, PCA revealed a broadly similar composition of these viral families across all continents, as indicated by overlapping clusters in the plot (Fig. 5a). The largest differences were observed for the *Astroviridae* and *Picornaviridae* families. However, at the genus level, more distinct differences in viral composition were observed between continents (Fig. 5b). Notably, Europe and Africa showed overlapping compositions, while the dataset for Oceania was distinctly separated. At the city level, even for the biannually sampled cities, PCA revealed clear distinct clustering, indicating significant variation in viral compositions between cities (Fig. 5c, d, Supplementary Fig. 5). These analyses identified the genus *Mamastrovirus* (*Astroviridae*) as the primary driver of beta-diversity. *Norovirus* and *Sapovirus* showed covariation, as reflected by the small angle between their loading vectors,

indicating similar contributions to the observed variation. Within the *Picornaviridae* family, genera such as *Enterovirus*, and *Cardiovirus*, also displayed some degree of covariation. The cities with longitudinal sampling showed that over time, Seattle (USA) and Copenhagen (Denmark) exhibited tightly clustered sample groupings at the family level, suggesting a stable composition of enteric virus families throughout the study period. In contrast, the virome composition in Regina (Canada), Kuala Lumpur (Malaysia), Guangzhou (China), and Yaoundé (Cameroon) showed greater variability, reflecting a more dynamic and heterogeneous composition over time. At the genus level, the enteric virome composition in Melbourne (Australia) was distinct from that of all other cities, primarily due to a high abundance of *Mamastroviruses* which may reflect differences in interregional connectivity (Fig. 5d).



Fig. 6 | Global prevalence and abundance of species within the *Tobamovirus* genus in urban wastewater. Biannual (a) and longitudinal data (b) are shown. In each panel, stacked bar plots display the number of reads per million viral reads assigned to the *Tobamovirus* genus (green) and to specific species (red), followed by the relative abundances of *Tobamovirus* species. The biannual samples were grouped using hierarchical clustering based on species-level composition. YoMV Youcai mosaic virus, TVCV Turnip VeinClearing virus, TSAMV Tropical soda

apple mosaic virus, ToMV Tomato mosaic virus, ToMMV Tomato mottle mosaic virus, TMV Tobacco mosaic virus, TMGMV Tobacco mild green mosaic virus, TBRFV Tomato brown rugose virus, RMV Ribgrass mosaic virus, RheMV Rehmannia mosaic virus, PMMoV Pepper mild mottle virus, PaMMV Paprika mild mottle virus, HLSV Hibiscus latent Singapore virus, HLFPV Hibiscus latent Fort Pierce virus, CMoV Cucumber mottle virus, CGMMV Cucumber green mild mottle virus, BPMV Bell pepper mottle virus, SA South America.

Species and genotype-level analysis of selected viral genera

We further explored the value of wastewater for monitoring viruses at finer taxonomic resolution, at the level of species and genotypes to capture fine-scale spatiotemporal patterns of viral diversity. The genera *Tobamovirus* (*Virgaviridae*) from the metagenomic sequence data and *Mamastrovirus* (*Astroviridae*) and *Enterovirus* (*Picornaviridae*) from the GastroCap data had the largest influence on virome compositions across the biannual samples in the PCA. Due to their relevance to plant, public, and animal health, these genera were selected for further investigation.

Shotgun metagenomic sequencing reveals *Tobamovirus* diversity in wastewater

Tobamoviruses are of major concern because they can cause disease in a wide range of agriculturally important plant species, affecting tomato, pepper and cucumber plants. We identified a total of 5204 *Tobamovirus* contigs in the metagenomic dataset of which 32% (1653 contigs) were assigned to 17 different species (Fig. 6), including both widely distributed, well-known viruses and emerging viruses with increasing agricultural and environmental relevance. Analysis of the sequences at the species level showed large compositional differences between samples and locations. Overall *Cucumber green mild mottle virus* (CGMMV) and *Pepper mild mottle virus* (PMMoV) – both well-studied and widely distributed viruses – were highly prevalent in urban sewage samples worldwide. PMMoV did not exhibit temporal variation,

but its relative abundance was lower in Asia (Fig. 6a, b). The relative abundance of CGMMV was highest in samples from Europe, Asia and North America (Fig. 6a, b). *Tobacco mosaic virus* (TMV) was predominantly found in high abundance in samples from Asia and Africa, while *Tobacco mild green mosaic virus* (TMGMV) was primarily observed in samples from Asia (Fig. 6a, b). Additionally, we detected emerging viruses of concern, such as the rapidly spreading *Tomato brown rugose fruit virus* (ToBRFV), which was detected in wastewater samples from multiple locations including Rome (Italy) in 2017 and Athens (Greece), Vancouver (Canada), Be'er Sheva (Israel) and Seattle (USA) in 2018 (Fig. 6a, b).

Global diversity and phylogenetic analysis of *Mamastrovirus* in wastewater

Variation in the relative abundance of the genus *Mamastrovirus* contributed most to the differentiation of samples in the PCA in the GastroCap sequence dataset (Fig. 5b). To explore if these differences were associated to specific *Mamastrovirus* types, we developed a custom typing workflow using reference sequences from a phylogenetic study on astrovirus diversity³³. Our approach identified 10,668 *Mamastrovirus* contigs of which 14% (1512 contigs) could be assigned a genotype, resulting in the detection of 24 different types. Our analysis revealed both well-established (endemic) and less commonly observed *Mamastrovirus* genotypes across various global wastewater samples. There was substantial variation in *Mamastrovirus* genotype



Fig. 7 | Global prevalence and abundance of *Mamastrovirus* genotypes in urban wastewater. Biannual (a) and longitudinal data (b) are shown. In each panel, stacked bar plots display the number of reads per million viral reads assigned to the *Mamastrovirus* genus (green) and to specific genotypes (red), followed by the relative abundances of *Mamastrovirus* genotypes. The biannual samples were

grouped using hierarchical clustering based on genotype composition. HAsV Human Astrovirus, RAsV Rat astrovirus, CAsV Canine astrovirus, FAsV Feline astrovirus, ChAsV Cheetah astrovirus, YakAsV Yak astrovirus, Other genotypes detected in fewer than 4 samples.

distribution between samples. Compositional differences in genotypes did not clearly correlate with specific continents or cities in the biannual dataset (Fig. 7a). Human astroviruses (HAsV) formed the major fraction of *Mamastrovirus* genotypes detected, among these, the classical HAsV type 1–5 and 8 were most frequently detected. HAsV-1, a genotype considered endemic worldwide, was frequently detected across all sampled continents and was the predominant genotype in many samples. HAsV-8, a genotype rarely reported in clinical surveillance, was also detected in high relative abundance across all continents. Additionally, recently discovered ‘non-classical’ astroviruses, including MLB1, VAI/HMO-C, VA2/HMO-A and VA3/HMO-B were detected across multiple continents. Human astrovirus BF34, first identified and exclusively detected in Burkina Faso in 2010 (Africa), was detected in wastewater samples from Cameroon (February and March 2018), Austria (June and November 2018) and Uganda (July 2018) indicating its presence across multiple geographic regions in 2018. While less common in wastewater samples, animal astroviruses like, canine- (CAsV), rat astrovirus (RAsV) and feline astrovirus (FAsV) were detected across continents, with surprisingly high prevalence of CAsV in Regina, Canada. For the cities with longitudinal sampling, temporal shifts in the genotype distribution were observed. PCA analyses showed that *Mamastrovirus* was a major driver for the distinct clustering of Melbourne’s virome (Fig. 5d) with consistently high proportions of *Mamastrovirus* reads detected. In Melbourne HAsV-5 was more prevalent during 2017 and in early 2018, while

HAsV-1 was mainly prevalent during the remainder of 2018. Other cities also exhibited peaks in *Mamastrovirus* reads over the observation period, but the timing of these peaks varied across locations and was not linked to a specific genotype.

To investigate the global diversity and circulation patterns of the abundant ‘classical’ human astroviruses in greater detail, we conducted phylogenetic analysis. The retrieval of partial capsid sequences for HAsV type 1, 2, 3, 4, 5 and 8 (Fig. 8 and Supplementary Fig. 8) from wastewater considerably expands the number of available capsid sequences from previously underrepresented regions. For several types we observed wastewater-specific clusters, indicating that current clinical surveillance does not fully capture the diversity of HAsVs. Additionally, phylogenetic analysis revealed that integrating global wastewater sequences within a limited timeframe provided insights into country and city specific virus circulation. Viral sequences from the same city often clustered together, as did sequences from samples collected closer in time suggesting periodic circulation and replacement of viral lineages over time. Notably, evidence suggestive of region-specific virus circulation was observed for some African HAsV type 4, 5, and 8 clusters. For example, HAsV-5 wastewater sequences from Cameroon (2018), Senegal (2019), and human faecal sequences from Cameroon (2014) formed a distinct cluster. Similarly, a separate HAsV-8 cluster comprised of sequences from clinical samples from Cameroon from 2014 and wastewater sequences from Nigeria (2018) was observed.

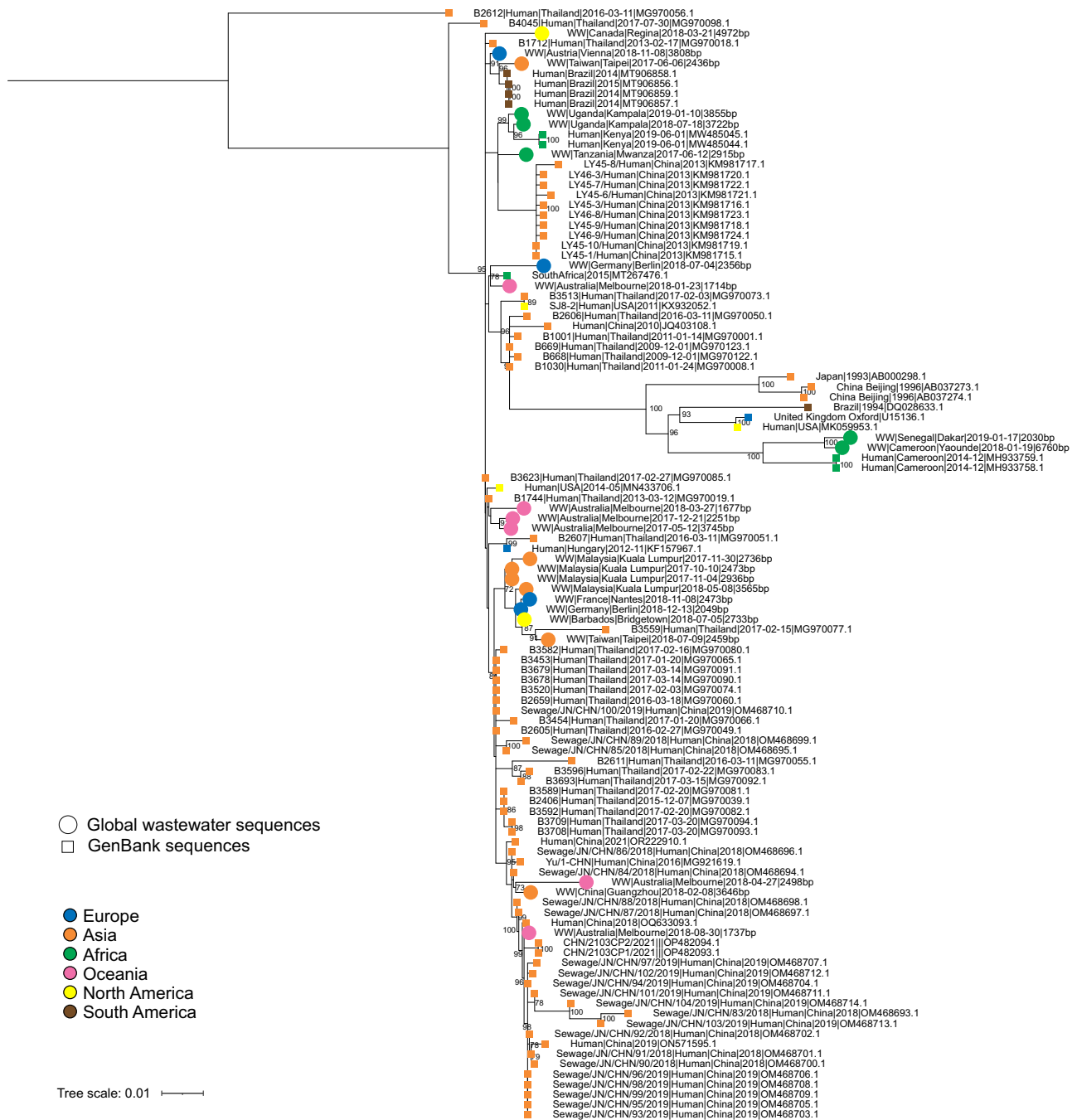


Fig. 8 | Phylogenetic analysis of Human astrovirus type 5 (HAstV-5) from global wastewater and publicly available reference sequences. Maximum likelihood phylogenetic tree of HAstV-5 based on partial ORF2 gene (capsid) sequences. Sequences obtained from GenBank are indicated in coloured squares, while

sequences derived from wastewater with a minimum length of 500 bp are denoted in coloured dots. Colours represent the continent of origin (Europe, Asia, Africa, Oceania, North America, and South America). Bootstrap values > 70 are shown.

Global diversity and phylogenetic analysis of enterovirus in wastewater

The abundance of *Picornaviridae* varied across continents, with enteroviruses frequently detected using GastroCap, significantly influencing PCA clustering patterns (Fig. 5d). Enteroviruses, a major public health concern due to their potential to cause a wide range of illnesses, including respiratory infections and neurological diseases, were analysed in wastewater to evaluate their surveillance potential in metagenomic datasets. A total of 2331 contigs were classified within the *Enterovirus* genus, of which 37% (868 contigs) could be genotyped using the RIVM Enterovirus genotyping tool, corresponding to 62 distinct *Enterovirus* genotypes.

Analysis of prevalence and relative abundance revealed differences in enterovirus distribution across continents (Fig. 9a, b). Samples from Africa showed the highest enterovirus abundance compared to other regions. *Enterovirus B* was the most prevalent species worldwide, with Coxsackievirus (CV) B5 and CV-A9 being the most prevalent types across all regions, suggesting widespread endemicity. In North America *Enterovirus A* was the most prevalent species, with Coxsackievirus CV-A6 and CV-A4, CV-A10 – endemic enteroviruses and common causes of hand, foot, and mouth disease- among the most detected types. *Enterovirus C*, though less prevalent, was frequently detected in the African region and was the dominant enterovirus species in longitudinal samples from Ecuador, Malaysia, and

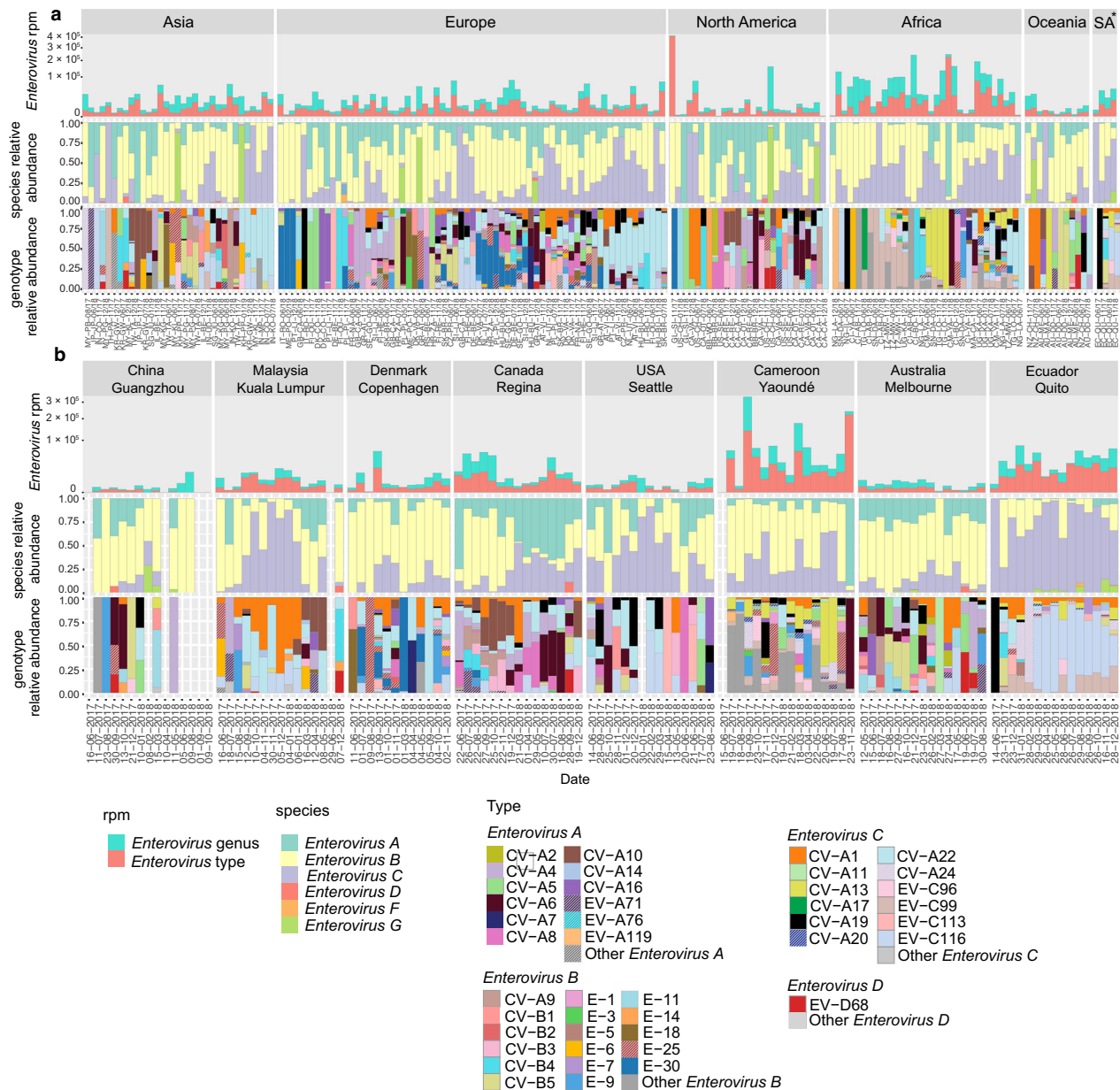


Fig. 9 | Global prevalence and abundance of Enterovirus genotypes in urban wastewater. Biannual (a) and longitudinal data (b) are shown. In each panel, stacked bar plots display reads per million viral reads assigned to the Enterovirus genus (green) and to specific genotypes (red), followed by the relative abundances

of Enterovirus species and of genotypes. The biannual samples were grouped using hierarchical clustering based on genotype composition. Other = genotypes detected in fewer than 10 samples, including (vaccine-derived) poliovirus type 3. SA South America.

Cameroon. While Enterovirus D was detected sporadically, Enterovirus D68—a clinically significant genotype due to its association with respiratory illness outbreaks and acute flaccid myelitis—was primarily identified toward the end of 2017 and in 2018. In most locations, Enterovirus D68 Clade B3 was predominant, while Clade A2 was detected in Athens and Taipei. Enterovirus G, associated with infection in pigs, was detected in high abundances in several cities across all continents.

Geographical specificity was evident for certain enterovirus genotypes. For example, CV-A20 was exclusively found in Africa and South America, while CV-A1 and CV-A22 were detected across all continents. In Europe, Echovirus type 30 (E-30) displayed an unusually high prevalence, which was not observed in other regions, possibly indicating a recent outbreak or re-emergence after a period of lower endemic circulation. Phylogenetic analysis of partial VP1 sequences

revealed that European wastewater E-30 sequences from 2018 were generally more closely related to each other than to sequences from 2017 (Fig. 10).

Longitudinal analysis revealed dynamic patterns in enterovirus genotype distribution across cities over time (Fig. 9b). For instance, Yaoundé (Cameroon) exhibited a broad diversity of circulating genotypes, including vaccine-derived poliovirus type 3. No sequences of the typing region VP1 for other polio types were detected. Longitudinal analysis across sites identified periods of genotype dominance, with CV-C116 – a lesser-known member of Enterovirus C with unknown clinical relevance – prevailing in Quito in 2018 and CV-A1 in Kuala Lumpur during 2017 and early 2018. In Regina, seasonal variations in overall enterovirus presence could be observed, with elevated levels occurring primarily during the summer and fall. Additionally, while multiple genotypes circulated in 2017, CV-A10 was present in higher

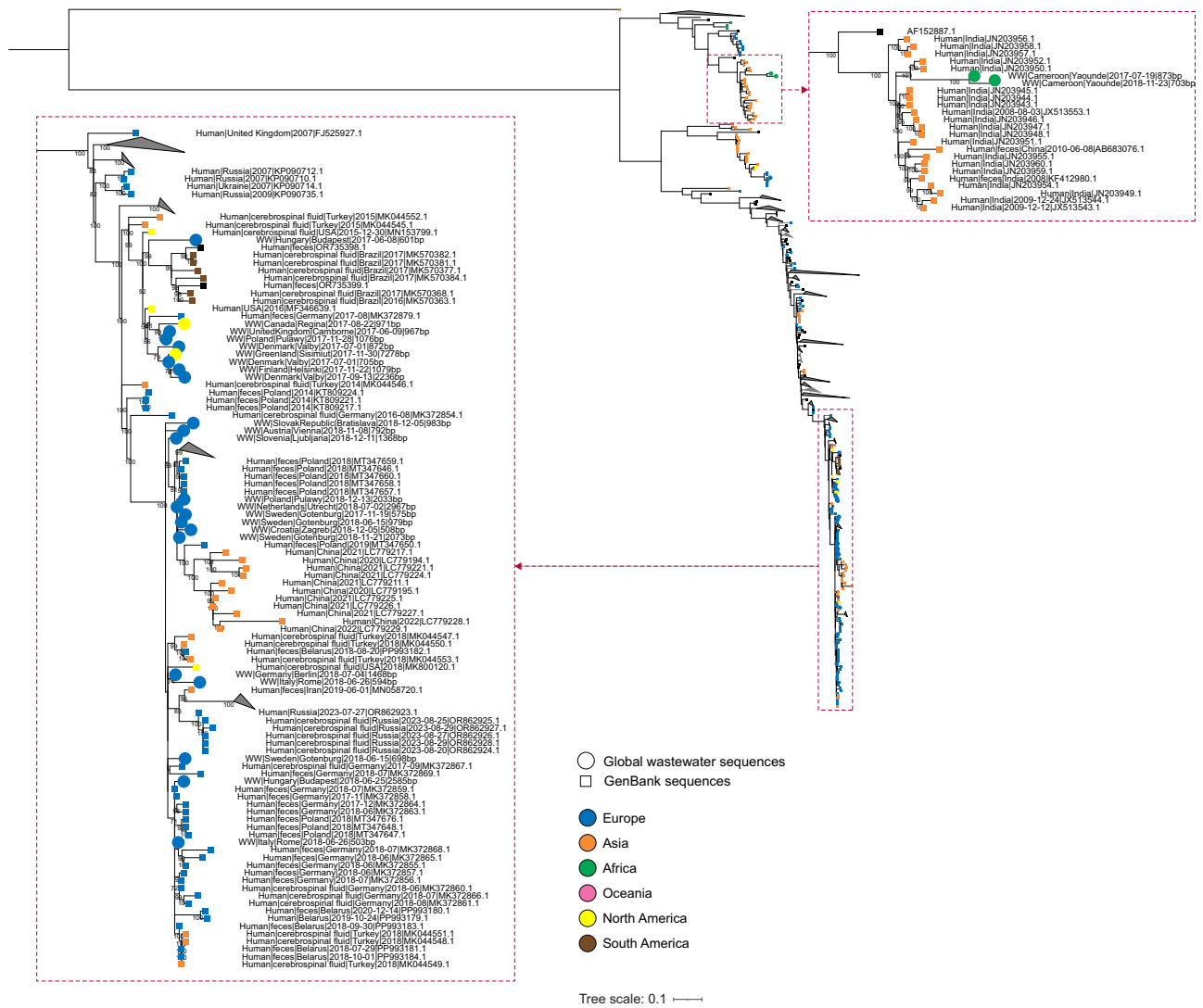


Fig. 10 | Phylogenetic analysis of Echovirus 30 (E30) from global wastewater and publicly available reference sequences. Maximum likelihood phylogenetic tree of E30 based on partial VP1 gene (capsid) sequences. Reference sequences obtained from GenBank are indicated with coloured squares, while sequences

derived from wastewater with a minimum length of 500 bp are denoted in coloured dots. Colours represent the continent of origin (Europe, Asia, Africa, Oceania, North America, and South America). Bootstrap values > 70 are shown.

relative abundance during specific periods, and shifted to CV-A6 in 2018, indicating dynamic changes in circulating enterovirus populations over consecutive years. Additionally, EV-A71 –one of the leading causes of hand, foot and mouth disease and associated with neurological complications - was detected in Regina in July, August and November 2017, coinciding with a period of elevated laboratory confirmed enterovirus/rhinovirus cases in Canada that year according to national surveillance data^{34,35}.

Discussion

This study provides a comprehensive analysis of the urban wastewater virome of 62 major cities worldwide using shotgun metagenomic and capture-based (GastroCap) sequencing. By incorporating both biannual and longitudinal samples, we assessed viral diversity and temporal dynamics. While biannual sampling provided a snapshot of viral diversity within a particular location, more frequent sampling revealed a higher viral diversity per location and enabled the detection of gradual shifts in composition. Shotgun metagenomics, at least with the sequencing depth used in our study, yielded a relatively low proportion of enteric virus reads, making it difficult to effectively monitor

enteric viruses in complex wastewater samples. The GastroCap probe set significantly enriched clinically relevant enteric viruses, whereas metagenomic sequencing primarily detected bacteriophages and plant viruses. Thus, for the surveillance of human pathogenic enteric viruses, which are stable in aquatic environments³⁶, wastewater is a valuable source when combined with GastroCap enrichment. Additionally, a large proportion of reads could not be assigned to known virus taxa, highlighting the potential for future discovery of novel viruses. Our findings and those of others demonstrate the utility of wastewater metagenomics as a powerful One Health surveillance tool, capturing the diversity and dynamics of viruses associated with human, animal, and environmental health.

Cross-continental comparisons revealed homogeneity in viral community composition at high taxonomic levels, consistent with findings that viral communities are often more specific to environmental habitats (e.g. wastewater or marine) rather than geographical location³⁷. At the city level, however, we observed geographical partitioning at both the family and genus levels, likely influenced by local factors such as climate, weather, demographics, agricultural practices, diet, population density and previous exposure history³⁰. Sampling in

South America, Central America and Oceania was limited, making the findings less generalizable for these regions. Additionally, an expanded dataset of these wastewater samples -sequenced using a strategy optimized for bacterial and AMR profiling- showed distinct regional variations in the resistome and bacteriome across continents. Specifically, bacterial composition divides the world's regions into roughly two major groups (Europe, Central Asia & North America versus Africa & Middle East), while the resistomes showed more unique regional profiles³¹. Our analysis revealed very limited antibiotic resistance gene (ARG) presence in the viral fraction, which may be due to the virus-enrichment protocol and the infrequent occurrence of ARGs by bacteriophage genomes³⁸ (Supplementary Table 1).

By increasing taxonomic resolution to the species and genotype level, our results and those of others demonstrate that metagenomic and phylogenetic analysis of viral communities in wastewater can reveal distinct temporal and geographical patterns³⁰. *Tobamoviruses* were highly prevalent in urban wastewater, consistent with their detection in various water sources^{39–41}. The widespread detection of CGMMV and PMMoV in our study align with their documented widespread prevalence^{42–44}. Notably, PMMoV has been proposed as a potential viral indicator for human faecal contamination in water and wastewater^{37,42,43}. However, our data showed significant regional variability, with lower proportions in Asia, suggesting that regional differences should be considered when interpreting PMMoV in water quality assessments. Variations in the composition of *Tobamovirus* species might reflect differences in agricultural practices or diet. For instance, the detection of TMGMV in China could be related to their substantial tobacco production and consumption^{45–47}. Importantly, early evidence of the emerging plant viruses like ToBRFV could also be detected. ToBRFV, which causes severe infections in tomatoes and peppers, was first described in Jordan in 2015, and retrospectively traced to Israel in 2014⁴⁸. Since then, it has spread widely, with our data indicating its presence in Canada as early as July 2018, more than a year before its first official report in 2019. Similarly, detections in Italy in November 2017 and in Greece in June 2018 precede their reported outbreaks by nearly a year^{49,50}. These findings highlight the utility of wastewater monitoring for the early detection and tracking of emerging plant pathogens.

Extending our study to viruses impacting animal and human health, we were able to characterize the diversity of astroviruses on a global scale. The prevalence and distribution of HAstV genotypes in our study generally align with trends observed in environmental, epidemiological, and serological studies. The detection of emerging viruses is an important focus of wastewater surveillance. In our study, 'non-classical' astroviruses, such as HAstV-MLB1, HAstV-VA1/HMO-C, HAstV-VA2/HMO-A, and HAstV-VA3/HMO-C which are sometimes associated with neurological disease in immunocompromised individuals⁵¹ were detected. Consistent with clinical reports indicating that non-classical astroviruses generally have lower detection rates than classical HAstVs, our wastewater data reflect this pattern with fewer samples positive for HAstV-MLB1 and a lower relative abundance compared to classical HAstVs^{51,52}. However, in certain samples, non-classical astroviruses were the predominant type, which may contribute to the high seroprevalences observed in seroepidemiological studies^{53,54}. An earlier metagenomic wastewater study reported higher abundances of astroviruses in the northern hemisphere during winter compared to the southern hemisphere⁵⁵, and seasonal peaks in HAstV infections have been observed in colder months in regions such as China, Spain, and the USA^{56–58}. However, comprehensive understanding of astrovirus types and their seasonality remains limited, and it is unclear whether types are constantly prevalent throughout the year or if they disappear and re-emerge over time⁵². Our findings showed consistent detection of some astroviruses like HAstV-1 in most locations with longitudinal sampling, while other types such as MLB1, were only detected in specific months (Fig. 7b). These findings suggest

that astrovirus seasonality may be type specific. The type specific differences observed in our study may reflect a complex interplay of viral characteristics (e.g. shedding duration, tropism), host population characteristics (e.g. population immunity, age distribution), and environmental factors (e.g. temperature, humidity, rainfall)^{57–60}.

Like astroviruses, enteroviruses have a major impact on public health, and polioviruses were the earliest viruses to be monitored in wastewater. Across our globally distributed wastewater samples, enterovirus abundance consistently showed a dominance of *Enterovirus B* across most regions, and high abundance of *Enterovirus C* types in African wastewater samples, aligning with trends from clinical surveillance^{60,61}. In contrast, *Enterovirus A* types, such as CV-A6 and CV-A10, which are frequently reported in clinical samples from Asia, were not dominant in wastewater from this region⁶⁰, potentially reflecting biases in clinical surveillance efforts that are targeted towards detection of the enterovirus types causing hand, foot, and mouth disease. EV-D68, another focus of clinical surveillance, was infrequently detected, possibly due to its respiratory transmission route and limited faecal shedding⁶². Its biennial circulation patterns, with even-numbered years from 2014 to 2018 in temperate climates^{63,64}, were reflected in our data, in which we detected EV-D68 primarily in 2018. Unlike some other viruses, wastewater detections of EV-D68 coincided with, rather than preceded, the timing of clinically recognized circulation. These findings suggest that the potential of wastewater metagenomics for early detection varies by virus and is influenced by biological factors, such as shedding dynamics, stability, and transmission mode, as well as clinical surveillance-related factors. Dynamic changes in enterovirus populations over time could be observed, including for genotypes not commonly detected in clinical surveillance, giving a broader perspective on circulating diversity. In many cases we only recovered partial genomes, complicating taxonomic annotation and limiting the ability to determine the clade, type, subtype or lineage which are often necessary to investigate outbreaks^{65,66}. For example, poliovirus type 3 detected in Cameroon likely reflects shedding of oral polio vaccine (OPV3) strains, which can, in rare cases, mutate into vaccine-derived polioviruses (VDPVs) capable of causing outbreaks. However, insufficient genomic resolution in critical regions (e.g., VP1, 5'UTR) prevented confirmation of whether the detected sequences represented vaccine strains or VDPVs.

Wastewater monitoring also captured emerging enteroviruses, exemplified by *Enterovirus E30*. High proportions of E30 were observed in European samples, aligning with increased reporting of E30 across European countries from 2015–2017⁶⁷, and a subsequent rise in meningitis and meningoencephalitis cases from April to September 2018⁶⁸. Notably, the detection of E30 in European wastewater as early as June 2017 preceded the clinical observations, suggesting undetected circulation before its recognized outbreak. These findings demonstrate that wastewater monitoring provides a comprehensive view of enterovirus diversity, geographical spread, and temporal changes, enabling the detection of both clinically targeted and undersurveilled types and the (re)emergence of specific genotypes.

Interestingly, animal-associated viruses were frequently detected in our dataset, including canine- and feline astrovirus and porcine enterovirus G, likely reflecting contamination from pet waste or animal industry runoff entering sewage systems. The high abundance of canine astrovirus in Regina (Canada) may be linked to local practices encouraging the flushing of dog waste into sewage systems, a method recommended in several Canadian cities since 2017 to reduce environmental pollution⁶⁹.

In conclusion, in this study, shotgun metagenomic and capture-based sequencing of wastewater provided insights into the genetic diversity and spatiotemporal patterns of both endemic and emerging viruses. In resource-limited settings, where clinical testing facilities and surveillance infrastructure may be constrained, centralized metagenomic wastewater-based monitoring could provide a cost-effective

and scalable alternative to detect viral threats. These findings underscore the value of wastewater metagenomic analysis as a One Health resource, offering insights into infectious disease dynamics.

Methods

Urban wastewater sample collection

Raw wastewater samples were collected from 62 sites from 6 continents as previously described⁷⁰. Briefly, unfiltered urban wastewater samples prior to the inlet of the wastewater treatment plant or main outlet to rivers were acquired. Where possible, flow proportion sampling over 24 h or otherwise three crude point samples were obtained for representative sampling. Samples were stored at -80°C and shipped. Additional metadata containing details on the sampling location and the conditions of the samples such as temperature and sample consistency were gathered. The biannual samples were obtained around June and November in 2017 and 2018 (and in some cases early 2019). Monthly longitudinal samples were collected from eight locations across six continents during the same period. The map showing the sampling locations was generated in R using the tidygeocoder package (version 1.0.6)⁷¹, and geocoded coordinates were obtained via the OpenStreetMap Nominatim API⁷².

Sample processing

Samples were thawed at room temperature and 50 ml of raw wastewater was centrifuged at $3744 \times g$ for 15 min to remove large debris. The supernatant was filtered using $0.45\ \mu\text{m}$ pore diameter filter to remove bacterial and eukaryotic cells. Although $0.22\ \mu\text{m}$ filters are also used in virome studies, they have been associated with reduced recovery of certain viral families and were therefore not used in this study⁷³. A volume of 30 mL of filtered supernatant was concentrated using 30 kDa Pierce™ Protein Concentrators PES (Thermo Fisher Scientific) by sequential centrifugation at $6000 \times g$ at 4°C (15 min for the initial 15 mL, followed by 30 min for the second 15 mL added to the same concentrator). The filtrate was treated with OmniCleave™ Endonuclease (Lucigen Corporation) for the removal of extracellular nucleic acid (Supplemental Fig. S9). Total nucleic acid content was extracted with the High Pure Viral Nucleic Acid Kit, without the use of DNase treatment (Roche).

Metagenomic and capture-based sequencing

Library preparation was done using the KAPA HyperPlus kit (Roche) using Superscript IV and random priming to synthesize cDNA from RNA. Subsequently, double-stranded DNA (dsDNA) was generated using Klenow and the samples were subjected to enzymatic fragmentation. End repair and A-tailing was performed and KAPA Dual Indexed adaptors were ligated. A post-ligation cleanup step was done using $0.8 \times$ AMPure XP Beads (Beckman Coulter). After that, a double-sided size selection was performed according to the manufacturer's instruction. Library PCR amplification was conducted using a total of 24 cycles. After purification, the quantity and quality assessment of the libraries was carried out using a Qubit 4 Fluorometer (Thermo Fisher Scientific) and an Agilent 2100 Bioanalyzer, following the respective manufacturers' protocols. The samples were pooled in equimolar proportions and sequenced directly or used as input for the GastroCap following sequencing on the Illumina MiSeq platform to generate 2×300 nt paired end sequences.

For target enrichment the GastroCap probe set was used. This probe set was designed to target a manually curated list of vertebrate virus species belonging to the *Adenoviridae*, *Astroviridae*, *Caliciviridae*, *Hepeviridae*, *Parvoviridae*, *Picornaviridae*, *Sedoreoviridae* and *Spinareoviridae* families (Supplementary Fig. 1). The probes were based on all sequences available in GenBank >500 nucleotides for the selected species. To minimize redundancy, sequences were clustered at 95% nucleotide identity. To enhance representation of less abundant viral species, sequences from genera other than the highly abundant

Enterovirus, *Mastadenovirus*, and *Rotavirus* were 'boosted' by multiplying their sequence abundance by a factor of three in the input dataset.

The GastroCap probe set was designed by Roche using their proprietary Nimble Design workflow. Six library samples were pooled in equimolar amounts and purified using AMPure XP Beads of the KAPA HyperCapture Bead kit (Roche). The GastroCap probes were diluted 1:10, and 4.5 mL was added to 10.5 mL of the sample pools. Hybridization was performed by incubating the samples at 95°C for 5 min and then at 47°C for 72 h. Following hybridization, 50 mL capture beads from the KAPA HyperCapture Bead kit (Roche) were washed according to the manufacturer's protocol, added to the hybridized sample pools (15 mL) and incubated at 47°C for 15 min. The sample pools were then washed, and a post-capture PCR was performed using 14 cycles before purification by AMPure XP Beads. The quantity and quality of the captured library pools were assessed using the Qubit 4 Fluorometer and the Agilent 2100 Bioanalyzer following the manufacturers' protocols. The capture reactions were then pooled equimolarly and sequenced on the Illumina MiSeq platform to generate 2×300 nt paired end sequences. To monitor potential contamination and technical consistency, we included negative controls and resequenced one sample as a technical replicate for each batch. As shown in Supplementary Fig. 9, replicates with similar read depth exhibited comparable taxonomic composition.

Sequence data analysis

The sequence analysis workflow was generated using Snakemake (version 7.19.1)⁷⁴. Raw fastq files were quality trimmed using FastP (version 0.23.4)⁷⁵. Read ends were trimmed to a mean quality Phred score of 25 with a sliding window of 5. Reads shorter than 30 nucleotides were discarded as well as reads with an average Phred score below 25. To identify and remove PCR duplicates, sequencing reads were deduplicated using CD-HIT⁷⁶, which groups and removes duplicate reads that are identical within the first 150 nucleotides. Reads were aligned to the GRCh38 human genome reference (version GCF_000001405.26) using BWA-MEM (version 0.7.17)⁷⁷ and filtered using SAMtools (version 1.6)⁷⁸ before the reads were assembled using metaSPAdes (version SP)⁷⁹. Taxonomic annotation was performed using DIAMOND v2.1.10.164⁸⁰ using the NCBI non-redundant protein reference database. Taxonomic assignment of each assembled contig was done based on the highest bit score normalized by the length of the contig. Finally, reads were mapped to the contigs using BWA-MEM to obtain read counts. Additionally, viral contigs ≥ 300 bp were screened for antimicrobial resistance genes (ARGs) and prophages using geNomad (version 1.11.0)⁸¹ with default settings. No prophages were detected, and only three contigs contained ARG annotations (Supplementary table 1).

Quantitative analysis: heatmaps of viral diversity

For further quantitative analysis, annotated contigs with a length ≥ 300 nucleotides and an average depth of coverage ≥ 3 were selected to ensure the inclusion of more reliable hits. The total number of reads assigned to the superkingdom "Viruses" per sample was used to normalize read counts. The total number of reads mapping to a contig (forward and or reverse) were adjusted by dividing by the average genome size per individual viral family. For viral families with large variation in genome sizes the average genus level genome size was used.

Relative viral abundance was calculated as reads per million (RPM) according to Eq. 1:

$$\text{Relative abundance} = \frac{\text{virus reads}}{\text{average genome length} \times \text{total viral reads}} * 10^6 \quad (1)$$

The classification of viral families based on their hosts range was obtained from Virus-Host DB, which pairs viruses and hosts using NCBI taxonomy IDs, integrating host information from genome databases like RefSeq and GenBank, along with additional sources including UniProt, ViralZone, and literature⁸².

Comparison of viral composition

We compared viral composition across different locations using PCA, accounting for the compositional nature of metagenomic data. Therefore, the Centred Log-Ratio (CLR) coefficients were computed for distinct data subsets to preserve the relative relationships between viral taxa⁸³. PCA was conducted on the viral fraction of the dataset using genome-size adjusted read counts to calculate CLR values. This normalization was not applied to plots at the superkingdom level (Archaea, Bacteria, Eukaryota (human separate), Viruses and Unknown) due to significant variability in genome sizes at this taxonomic level. For the virome data at family, genus and species level (metagenomic sequence data), only viral taxa with a high CLR median and high variance were retained, excluding those with low abundance and minimal variability between samples. PCA was also performed separately for DNA and RNA viruses to explore potential differences in community composition between viral genome types.

For enteric viruses, all viral families targeted by the GastroCap probe set were included without additional filtering. Zero values were replaced using an Aitchison mean point estimate before applying the CLR transformation. The transformed data were then visualized in a biplot using the pyCoDaMath package in Python (version 3.8).

Taxonomic analysis at the species and genotype level for selected viruses

For selected viruses, the dataset was filtered to extract contigs belonging to specific genera using DIAMOND annotation with a contig length ≥ 300 and average depth of coverage of $\geq 3\times$. These contigs were then processed using custom workflows to determine species and genotype. These workflows involved mapping contigs with a blast search against a database of reference sequences from literature or existing typing tools, and assigning species and type based on virus specific ICTV classification criteria.

Tobamovirus species assignment

A custom blastn species assignment database was generated using sequences from all 37 ICTV-recognized *Tobamovirus* species. Contigs were assigned to specific species based on the criterion that strains within the same species must share >300 bp and 90% nucleotide sequence identity across the whole genome, following the species demarcation criteria proposed by ICTV⁸⁴.

Mamastrovirus and Enterovirus genotyping and phylogenetic analysis

The typing workflow for *Mamastrovirus* used a nucleotide blast database of complete ORF2 sequences sourced from Donato et al.³³. Annotated *Mamastrovirus* contigs were aligned against this database using blastn. Contigs that covered at least 10% of ORF2 and exhibiting $\geq 85\%$ nucleotide identity, in line with classification criteria proposed by the ICTV Astroviridae Study Group^{52,85}, were included for further analysis. *Enterovirus* contigs were assigned using the RIVM enterovirus typing tool, which performs a blastn search and phylogenetic analysis of the (partial) VP1 gene, with a minimum overlap of 100 bp required for classification⁸⁶. For phylogenetic analysis, sequences covering >500 bp of ORF2 were considered sufficient for reliable alignment and tree-building. Complete and partial Human astrovirus (type 1-8) ORF2 sequences and E-30 VP1 sequences were retrieved from NCBI, combined with our sequences and aligned using MAFFT (version 7.508)⁸⁷. Phylogenetic trees were generated using IQ-TREE (version

2.3.6), using automated model selection, the -czb option, and 1000 bootstrap replicates⁸⁸.

Reporting summary

Further information on research design is available in the Nature Portfolio Reporting Summary linked to this article.

Data availability

The raw sequencing datasets, metagenome assemblies and analysis results are available on the European Nucleotide Archive under project: [PRJEB87273](https://www.ebi.ac.uk/ena/browser/view/PRJEB87273). Source data are provided with this paper.

Code availability

The metagenomic workflow used in this study is made available at https://github.com/EMC-Viroscience/Worp_etal_Global_Sewage_Virome⁸⁹.

References

- Meadows, A. J., Stephenson, N., Madhav, N. K. & Oppenheim, B. Historical trends demonstrate a pattern of increasingly frequent and severe spillover events of high-consequence zoonotic viruses. *BMJ Glob. Health* **8**, e012026 (2023).
- Neiderud, C. J. How urbanization affects the epidemiology of emerging infectious diseases. *Infect. Ecol. Epidemiol.* **5**, 27060 (2015).
- Alirol, E., Getaz, L., Stoll, B., Chappuis, F. & Loutan, L. Urbanisation and infectious diseases in a globalised world. *Lancet Infect. Dis.* **11**, 131 (2011).
- Bloomfield, L. S. P., McIntosh, T. L. & Lambin, E. F. Habitat fragmentation, livelihood behaviors, and contact between people and nonhuman primates in Africa. *Landsc. Ecol.* **35**, 985–1000 (2020).
- Daszak, P., Cunningham, A. A. & Hyatt, A. D. Emerging infectious diseases of wildlife - Threats to biodiversity and human health. *Science* **287**, 443–449 (2000).
- Rohr, J. R. et al. Emerging human infectious diseases and the links to global food production. *Nat. Sustain.* **2019** **2**, 445–456 (2019).
- Our World in Data & World Bank (UN Population Division). *Rural Population*. <https://ourworldindata.org/urbanization> (2024).
- Nieuwenhuijse, D. F. & Koopmans, M. P. G. Metagenomic sequencing for surveillance of food- and waterborne viral diseases. *Front Microbiol.* **8**, 242592 (2017).
- Thézé, J. et al. Genomic epidemiology reconstructs the introduction and spread of Zika virus in central America and Mexico. *Cell Host Microbe* **23**, 855–864.e7 (2018).
- Oude Munnink, B. B. et al. Rapid SARS-CoV-2 whole-genome sequencing and analysis for informed public health decision-making in the Netherlands. *Nat. Med.* **26**, 1405–1410 (2020).
- Medema, G., Heijnen, L., Elsinga, G., Italiaander, R. & Brouwer, A. Presence of SARS-coronavirus-2 RNA in sewage and correlation with reported COVID-19 prevalence in the early stage of the epidemic in the Netherlands. *Environ. Sci. Technol. Lett.* **7**, 511–516 (2020).
- Davis, J. T. et al. Cryptic transmission of SARS-CoV-2 and the first COVID-19 wave. *Nature* **2021** **600**, 127–132 (2021).
- Baz-Lomba, J. A. et al. Comparison of pharmaceutical, illicit drug, alcohol, nicotine and caffeine levels in wastewater with sale, seizure and consumption data for 8 European cities. *BMC Public Health* **16**, 1–11 (2016).
- Devault, D. A., Néfau, T., Pascaline, H., Karolak, S. & Levi, Y. First evaluation of illicit and licit drug consumption based on wastewater analysis in Fort de France urban area (Martinique, Caribbean), a transit area for drug smuggling. *Sci. Total Environ.* **490**, 970–978 (2014).
- Munk, P. et al. Genomic analysis of sewage from 101 countries reveals global landscape of antimicrobial resistance. *Nat. Commun.* **13**, 1–16 (2022).

16. Levy, J. I., Andersen, K. G., Knight, R. & Karthikeyan, S. Wastewater surveillance for public health. *Science* **379**, 26–27 (2023).
17. Schneider, J. et al. Detection of invasive mosquito vectors using environmental DNA (eDNA) from water samples. *PLoS One* **11**, e0162493 (2016).
18. Link-Gelles, R. et al. Public health response to a case of paralytic poliomyelitis in an unvaccinated person and detection of poliovirus in wastewater — New York, June–August 2022. *MMWR Morb. Mortal. Wkly Rep.* **71**, 1065–1068 (2022).
19. Klapsa, D. et al. Sustained detection of type 2 poliovirus in London sewage between February and July, 2022, by enhanced environmental surveillance. *Lancet* **400**, 1531–1538 (2022).
20. Duizer, E. et al. Wild poliovirus type 3 (WPV3)-shedding event following detection in environmental surveillance of poliovirus essential facilities, the Netherlands, November 2022 to January 2023. *Eurosurveillance* **28**, 2300049 (2023).
21. Izquierdo-Lara, R. et al. Monitoring SARS-CoV-2 circulation and diversity through community wastewater sequencing, the Netherlands and Belgium. *Emerg Infect. Dis* **27**, 1405–1415 (2021).
22. Jahn, K. et al. Early detection and surveillance of SARS-CoV-2 genomic variants in wastewater using COJAC. *Nat. Microbiol.* **2022**, 1151–1160 (2022).
23. Toribio-Avedillo, D. et al. Monitoring influenza and respiratory syncytial virus in wastewater. Beyond COVID-19. *Sci. Total Environ.* **892**, 164495 (2023).
24. Wolfe, M. K. et al. Use of wastewater for Mpox outbreak surveillance in California. *N. Engl. J. Med.* **388**, 570–572 (2023).
25. Lee, W. L. et al. Monitoring human arboviral diseases through wastewater surveillance: challenges, progress and future opportunities. *Water Res* **223**, 118904 (2022).
26. Tedcastle, A. et al. Detection of enterovirus D68 in wastewater samples from the UK between July and November 2021. *Viruses* **14**, 143 (2022).
27. Gibson, K. E. Viral pathogens in water: occurrence, public health impact, and available control strategies. *Curr. Opin. Virol.* **4**, 50–57 (2014).
28. Ko, K. K., Chng, K. R. & Nagarajan, N. Metagenomics-enabled microbial surveillance. *Nat. Microbiol.* **2022**, 486–496 (2022).
29. Harvey, E. & Holmes, E. C. Diversity and evolution of the animal virome. *Nat. Rev. Microbiol.* **2022**, 321–334 (2022).
30. Tisza, M. et al. Wastewater sequencing reveals community and variant dynamics of the collective human virome. *Nat. Commun.* **2023**, 1–10 (2023).
31. Munk, P. et al. Genomic analysis of sewage from 101 countries reveals global landscape of antimicrobial resistance. *Nat. Commun.* **13**, 7251 (2022).
32. Tuladhar, E. T. et al. Gemykibivirus detection in acute encephalitis patients from Nepal. *medRxiv* 15, 2024.02.13.24302648 (2024).
33. Donato, C. & Vijaykrishna, D. The broad host range and genetic diversity of mammalian and avian astroviruses. *Viruses* **2017**, 9, 102 (2017).
34. Public Health Agency of Canada. *Respiratory Virus Report, Week 34 Ending August 26, 2017*. <https://www.canada.ca/en/public-health/services/surveillance/respiratory-virus-detectionscanada/2016-2017/respiratory-virus-detections-isolations-week-34-ending-august-26-2017.html> (2018).
35. Public Health Agency of Canada. *Respiratory Virus Report, Week 34 Ending August 25, 2018*. <https://www.canada.ca/en/public-health/services/surveillance/respiratory-virus-detectionscanada/2017-2018/respiratory-virus-detections-isolations-week-34-ending-august-25-2018.html> (2021).
36. Fong, T.-T. & Lipp, E. K. Enteric viruses of humans and animals in aquatic environments: health risks, detection, and potential water quality assessment tools. *Microbiol. Mol. Biol. Rev.* **69**, 357 (2005).
37. Paez-Espino, D. et al. Uncovering Earth’s virome. *Nature* **536**, 425–430 (2016).
38. Enault, F. et al. Phages rarely encode antibiotic resistance genes: a cautionary tale for virome analyses. *ISME J.* **2017**, 237–247 (2016).
39. Haramoto, E. et al. Occurrence of pepper mild mottle virus in drinking water sources in Japan. *Appl Environ. Microbiol.* **79**, 7413–7418 (2013).
40. Jeżewska, M., Trzmiel, K. & Zarzyńska-Nowak, A. Detection of infectious tobamoviruses in irrigation and drainage canals in Greater Poland. *J. Plant Prot. Res.* **58**, 202–205 (2018).
41. Fernandez-Cassi, X. et al. Metagenomics for the study of viruses in urban sewage as a tool for public health surveillance. *Sci. Total Environ.* **618**, 870–880 (2018).
42. Vélez-Olmedo, J. B. et al. Tobamoviruses of two new species trigger resistance in pepper plants harbouring functional L alleles. *J. Gen. Virol.* **102**, 001524 (2021).
43. Kitajima, M., Sassi, H. P. & Torrey, J. R. Pepper mild mottle virus as a water quality indicator. *npj Clean. Water* **2018**, 1, 1–9 (2018).
44. Dombrovsky, A., Tran-Nguyen, L. T. T. & Jones, R. A. C. Cucumber green mottle mosaic virus: rapidly increasing global distribution, etiology, epidemiology, and management. *Annu. Rev. Phytopathol.* **55**, 231–256 (2017).
45. Asad, Z. et al. Genetic diversity of cucumber green mottle mosaic virus (CGMMV) infecting cucurbits. *Saudi J. Biol. Sci.* **29**, 3577–3585 (2022).
46. Food and Agriculture Organization of the United Nations. *Tobacco Production – FAO*. <https://ourworldindata.org/grapher/tobacco-production> (2023).
47. Ritchie, H. & Roser, M. Smoking. *Our World in Data* (2023).
48. Zhang, S., Griffiths, J. S., Marchand, G., Bernards, M. A. & Wang, A. Tomato brown rugose fruit virus: an emerging and rapidly spreading plant RNA virus that threatens tomato production worldwide. *Mol. Plant Pathol.* **23**, 1262 (2022).
49. Panno, S., Caruso, A. G. & Davino, S. First report of tomato brown rugose fruit virus on tomato crops in Italy. *APS* <https://doi.org/10.1094/PDIS-12-18-2254-PDN> (2019).
50. Beris, D. et al. *First Rep. Tomato Brown Rugose Fruit. Virus Infecting Tomato Greece* **104**, 2035, <https://doi.org/10.1094/PDIS-01-20-0212-PDN> (2020).
51. Vu, D. L., Cordey, S., Brito, F. & Kaiser, L. Novel human astroviruses: novel human diseases?. *J. Clin. Virol.* **82**, 56–63 (2016).
52. Vu, D. L., Bosch, A., Pintó, R. M. & Guix, S. Epidemiology of classic and novel human astrovirus: gastroenteritis and beyond. *Viruses* **9**, 33 (2017).
53. Holtz, L. R. et al. Seroepidemiology of astrovirus MLB1. *Clin. Vaccin. Immunol.* **21**, 908 (2014).
54. Burbelo, P. D. et al. Serological studies confirm the novel astrovirus HMOAstV-C as a highly prevalent human infectious agent. *PLoS One* **6**, e22576 (2011).
55. Nieuwenhuijse, D. F. et al. Setting a baseline for global urban virome surveillance in sewage. *Sci. Rep.* **2020**, 10, 1–13 (2020).
56. Guix, S. et al. Molecular epidemiology of astrovirus infection in Barcelona, Spain. *J. Clin. Microbiol.* **40**, 133–139 (2002).
57. Chhabra, P. et al. Etiology of viral gastroenteritis in children <5 Years of age in the United States, 2008–2009. *J. Infect. Dis.* **208**, 790–800 (2013).
58. Luo, X., Deng, J. kai, Mu, X. ping, Yu, N. & Che, X. Detection and characterization of human astrovirus and sapovirus in outpatients with acute gastroenteritis in Guangzhou, China. *BMC Gastroenterol.* **21**, 455 (2021).
59. Bosch, A., Pintó, R. M. & Guix, S. Human astroviruses. *Clin. Microbiol. Rev.* **27**, 1048–1074 (2014).
60. Brown, D. M., Zhang, Y. & Scheuermann, R. H. Epidemiology and sequence-based evolutionary analysis of circulating non-polio enteroviruses. *Microorganisms* **2020**, 8, 1856 (2020). Page.

61. Brouwer, L., Moreni, G., Wolthers, K. C. & Pajkrt, D. World-wide prevalence and genotype distribution of enteroviruses. *Viruses* **2021** *13*, 434 (2021).
62. Harvala, H. et al. Recommendations for enterovirus diagnostics and characterisation within and beyond Europe. *J. Clin. Virol.* **101**, 11–17 (2018).
63. Howson-Wells, H. C. et al. Enterovirus D68 epidemic, UK, 2018, was caused by subclades B3 and D1, predominantly in children and adults, respectively, with both subclades exhibiting extensive genetic diversity. *Microb. Genom.* **8**, mgen000825 (2022).
64. Park, S. W. et al. Epidemiological dynamics of enterovirus D68 in the United States and implications for acute flaccid myelitis. *Sci. Transl. Med.* **13**, eabd2400 (2021).
65. Arias, A. et al. Rapid outbreak sequencing of Ebola virus in Sierra Leone identifies transmission chains linked to sporadic cases. *Virus Evol.* **2**, vew016 (2016).
66. Masirika, L. M. et al. Ongoing mpox outbreak in Kamituga, South Kivu province, associated with monkeypox virus of a novel Clade I sub-lineage, Democratic Republic of the Congo, 2024. *Euro-surveillance* **29**, 2400106 (2024).
67. Bubba, L. et al. Circulation of non-polio enteroviruses in 24 EU and EEA countries between 2015 and 2017: a retrospective surveillance study. *Lancet Infect. Dis.* **20**, 350–361 (2020).
68. Broberg, E. K. et al. Upsurge in echovirus 30 detections in five EU/EEA countries, April to September, 2018. *Euro Surveill* **23**, 1800537 (2018).
69. City of North Vancouver. *Dog Waste Program*. <https://www.cnv.org/home-property/garbage-recyclinggreen-can/dog-waste-program> (2021).
70. Hendriksen, R. S. et al. Global monitoring of antimicrobial resistance based on metagenomics analyses of urban sewage. *Nat. Commun.* **10**, 1124 (2019).
71. Cambon, J., Hernangómez, D., Belanger, C. & Possenriede, D. tidygeocoder: an R package for geocoding. *J. Open Source Softw.* **6**, 3544 (2021).
72. OpenStreetMap contributors. *OpenStreetMap*. <https://www.openstreetmap.org> (2024).
73. Conceição-Neto, N. et al. Modular approach to customise sample preparation procedures for viral metagenomics: a reproducible protocol for virome analysis. *Sci. Rep.* **5**, 16532 (2015).
74. Köster, J. et al. Sustainable data analysis with Snakemake. *F1000Research* **2021** *10*, 33 (2021).
75. Chen, S., Zhou, Y., Chen, Y. & Gu, J. fastp: an ultra-fast all-in-one FASTQ preprocessor. *Bioinformatics* **34**, i884–i890 (2018).
76. Fu, L., Niu, B., Zhu, Z., Wu, S. & Li, W. CD-HIT: accelerated for clustering the next-generation sequencing data. *Bioinformatics* **28**, 3150 (2012).
77. Li, H. & Durbin, R. Fast and accurate short read alignment with Burrows–Wheeler transform. *Bioinformatics* **25**, 1754–1760 (2009).
78. Li, H. et al. The sequence alignment/map format and SAMtools. *Bioinformatics* **25**, 2078–2079 (2009).
79. Nurk, S., Meleshko, D., Korobeynikov, A. & Pevzner, P. A. MetaSPAdes: A new versatile metagenomic assembler. *Genome Res.* **27**, 824–834 (2017).
80. Buchfink, B., Xie, C. & Huson, D. Fast and sensitive protein alignment using DIAMOND. *Nat Methods* **12**, 59–60 (2015).
81. Camargo, A. P. et al. Identification of mobile genetic elements with geNomad. *Nat. Biotechnol.* **2023** *42*, 1303–1312 (2023).
82. Mihara, T. et al. Linking virus genomes with host taxonomy. *Viruses* **8**, 66 (2016).
83. Gloor, G. B., Macklaim, J. M., Pawlowsky-Glahn, V. & Egozcue, J. J. Microbiome datasets are compositional: and this is not optional. *Front Microbiol.* **8**, 294209 (2017).
84. Adams, M. J. et al. ICTV Virus taxonomy profile: virgaviridae. *J. Gen. Virol.* **98**, 1999–2000 (2017).
85. King, A. M. Q., Lefkowitz, Elliot., Adams, M. J. & Carstens, E. B. *Virus Taxonomy: Ninth Report of the International Committee on Taxonomy of Viruses*, Vol. 1462 (Elsevier Science, 2011).
86. Kroneman, A. et al. An automated genotyping tool for enteroviruses and noroviruses. *J. Clin. Virol.* **51**, 121–125 (2011).
87. Katoh, K., Misawa, K., Kuma, K. I. & Miyata, T. MAFFT: a novel method for rapid multiple sequence alignment based on fast Fourier transform. *Nucleic Acids Res.* **30**, 3059–3066 (2002).
88. Nguyen, L. T., Schmidt, H. A., Von Haeseler, A. & Minh, B. Q. IQ-TREE: A fast and effective stochastic algorithm for estimating maximum-likelihood phylogenies. *Mol. Biol. Evol.* **32**, 268 (2015).
89. Worp, N., Nieuwenhuijse, D. F. Unveiling the global urban virome by wastewater metagenomics. *Zenodo*. <https://doi.org/10.5281/zenodo.17095032> (2025).

Acknowledgements

This work has received funding from the European Union’s Horizon 2020 research and innovation program, project Veratile Emerging infectious disease Observatory (VEO) under grant agreement no. 874735 awarded to M.P.G.K and the NWO Stevin Prize 2018 awarded to M.P.G.K. by the Dutch Research Council (NWO).

Author contributions

M.P.G.K. and F.M.A. conceived the study, secured funding and provided overall supervision. M.G. & N.W. drafted the initial manuscript with input from M.P.G.K., M.G. & B.B.O.M. supervised manuscript preparation and data analysis. C.M.E.S. and N.W. performed NGS. N.W. and D.F.N. performed bioinformatic data analyses. E.E.B.J. and C.B. contributed to the PCA and provided methodological guidance. N.W. produced the figures. D.F.N., R.W.I.L., C.M.E.S., C.B., E.E.B.J., P.M., R.S.H., F.M.A., M.P.G.K., M.G. & B.B.O.M., critically read and contributed to the manuscript. The Global Sewage Consortium authors carried out sewage sampling, filled in metadata and shipped the samples.

Competing interests

The authors declare no competing interests.

Additional information

Supplementary information The online version contains supplementary material available at <https://doi.org/10.1038/s41467-025-65208-x>.

Correspondence and requests for materials should be addressed to Miranda de Graaf.

Peer review information *Nature Communications* thanks Miguel Uya-guari-Diaz, and the other, anonymous, reviewers for their contribution to the peer review of this work. A peer review file is available.

Reprints and permissions information is available at <http://www.nature.com/reprints>

Publisher’s note Springer Nature remains neutral with regard to jurisdictional claims in published maps and institutional affiliations.

Open Access This article is licensed under a Creative Commons Attribution-NonCommercial-NoDerivatives 4.0 International License, which permits any non-commercial use, sharing, distribution and reproduction in any medium or format, as long as you give appropriate credit to the original author(s) and the source, provide a link to the Creative Commons licence, and indicate if you modified the licensed material. You do not have permission under this licence to share adapted material derived from this article or parts of it. The images or other third party material in this article are included in the article's Creative Commons licence, unless indicated otherwise in a credit line to the material. If material is not included in the article's Creative Commons licence and your intended use is not permitted by statutory regulation or exceeds the permitted use, you will need to obtain permission directly from the copyright holder. To view a copy of this licence, visit <http://creativecommons.org/licenses/by-nc-nd/4.0/>.

© The Author(s) 2025

Global Sewage Surveillance Consortium

Frederik Duus Møller², Thomas N. Petersen², Jette S. Kjeldgaard², Christina Aaby Svendsen², Artan Bego⁴, Pablo Power⁵, Catherine Rees⁶, Dionisia Lambrinidis⁷, Elizabeth Heather Jakobsen Neilson⁸, Karen Gibb⁹, Kris Coventry⁶, Peter Collignon¹⁰, Susan Cassar¹¹, Franz Allerberger¹², Anowara Begum¹³, Zenat Zebin Hossain¹³, Carlton Worrell¹⁴, Olivier Vandenberg¹⁵, Ilse Pieters¹⁶, Dougnon Tamègnon Victorien¹⁷, Angela Daniela Salazar Gutierrez¹⁸, Freddy Soria¹⁸, Vesna Rudić Grujić¹⁹, Nataša Mazalica²⁰, Teddie O. Rahube²¹, Carlos Alberto Tagliati²², Dalia Rodrigues²³, Guilherme Oliveira²⁴, Larissa Camila Ribeiro de Souza²², Ivan Ivanov²⁵, Bonkoungou Isidore Juste²⁶, Traoré Oumar²⁶, Thet Sopheak²⁷, Yith Vuthy²⁷, Antoinette Ngandjio²⁸, Ariane Nzouankeu²⁸, Ziem A. Abah Jacques Olivier²⁸, Christopher K. Yost²⁹, Pratik Kumar³⁰, Satinder Kaur Brar³¹, Djim-Adjim Tabo³², Aiko D. Adell³³, Esteban Paredes-Osses³⁴, Maria Cristina Martinez³⁴, Sara Cuadros-Orellana³⁵, Changwen Ke³⁶, Huanying Zheng³⁶, Li Baisheng³⁶, Lok Ting Lau³⁷, Teresa Chung³⁷, Xiaoyang Jiao³⁸, Yongjie Yu³⁹, Zhao JiaYong⁴⁰, Johan F. Bernal Morales⁴¹, Maria Fernanda Valencia⁴¹, Pilar Donado-Godoy⁴¹, Kalpy Julien Coulibaly⁴², Jasna Hrenovic⁴³, Matijana Jergović⁴⁴, Renáta Karpíšková⁴⁵, Zozo Nyarukweba Deogratias⁴⁶, Bodil Elsborg⁴⁷, Lisbeth Truelstrup Hansen⁴⁸, Pernille Erland Jensen⁴⁸, Mohamed Abouelnaga⁴⁹, Mohamed Fathy Salem⁵⁰, Marliin Koolmeister⁵¹, Mengistu Legesse⁵², Tadesse Eguale⁵², Annamari Heikinheimo⁵³, Soizick Le Guyader⁵⁴, Julien Schaeffer⁵⁴, Jose Eduardo Villacis⁵⁵, Bakary Sanneh⁵⁶, Lile Malania⁵⁷, Andreas Nitsche⁵⁸, Annika Brinkmann⁵⁸, Sara Schubert⁵⁹, Sina Hesse⁵⁹, Thomas U. Berendonk⁵⁹, Courage Kosi Setsoafia Saba⁶⁰, Jibril Mohammed⁶¹, Patrick Kwame Feglo⁶², Regina Ama Banu⁶³, Charalampos Kotzamanidis⁶⁴, Efthymios Lytras⁶⁵, Sergio A. Lickes⁶⁶, Bela Kocsis⁶⁷, Norbert Solymosi⁶⁸, Thorunn R. Thorsteinsdottir⁶⁹, Abdulla Mohamed Hatha⁷⁰, Mamatha Ballal⁷¹, Sohan Rodney Bangera⁷², Fereshteh Fani⁷³, Masoud Alebouyeh⁷⁴, Dearbhaile Morris⁷⁵, Louise O'Connor⁷⁵, Martin Cormican⁷⁵, Jacob Moran-Gilad⁷⁶, Antonio Battisti⁷⁷, Elena Lavinia Diaconu⁷⁷, Gianluca Corno⁷⁸, Andrea Di Cesare⁷⁸, Patricia Alba⁷⁷, Junzo Hisatsune⁷⁹, Liansheng Yu⁷⁹, Makoto Kuroda⁷⁹, Motoyuki Sugai⁷⁹, Shizuo Kayama⁷⁹, Zeinegul Shakenova⁸⁰, Ciira Kiiyukia⁸¹, Eric Ng'eno⁸², Lul Raka⁸³, Kazi Jamil⁸⁴, Saja Adel Fakhraldeen⁸⁴, Tareq Alaati⁸⁴, Aivars Bērziņš⁸⁵, Jeļena Avsejenko⁸⁵, Kristina Kokina⁸⁵, Madara Streikisa⁸⁵, Vadims Bartkevics⁸⁵, Ghassan M. Matar⁸⁶, Ziad Daoud⁸⁷, Asta Pereckienė⁸⁸, Ceslova Butrimaite-Ambrozeviciene⁸⁸, Christian Penny⁸⁹, Alexandra Bastarud⁹⁰, Tiavina Rasolofoarison⁹¹, Jean-Marc Collard⁹⁰, Luc Hervé Samison⁹¹, Mala Rakoto Andrianarivelo⁹¹, Daniel Lawadi Banda⁹², Arshana Amin⁹³, Heraa Rajandas⁹⁴, Sivachandran Parimannan⁹⁴, David Spiteri⁹⁵, Malcolm Vella Haber⁹⁶, Sunita J. Santchurn⁹⁷, Aleksandar Vujacic⁹⁸, Dijana Djurovic⁹⁸, Brahim Bouchrif⁹⁹, Bouchra Karraouan⁹⁹, Delfino Carlos Vubil¹⁰⁰, Pushkar Pal¹⁰¹, Heike Schmitt¹⁰², Mark van Passel¹⁰², Gert-Jan Jeunen¹⁰³, Neil Gemmell¹⁰³, Stephen T. Chambers¹⁰⁴, Fania Perez Mendoza¹⁰⁵, Jorge Huete-Perez¹⁰⁵, Samuel Vilchez¹⁰⁶, Akeem Olayiwola Ahmed¹⁰⁷, Ibrahim Raufu Adisa¹⁰⁷, Ismail Ayoade Odetokun¹⁰⁷, Kayode Fashae¹⁰⁸, Anne-Marie Sørgaard¹⁰⁹, Astrid Louise Wester¹⁰⁹, Pia Ryrfors¹¹⁰, Rune Holmstad¹¹⁰, Mashkoor Mohsin¹¹¹, Rumina Hasan¹¹², Sadia Shakoor¹¹², Natalie Weiler Gustafson¹¹³, Claudia Huber Schill¹¹³, Maria Luz Zamudio Rojas¹¹⁴, Jorge Echevarria Velasquez¹¹⁵, Bonifacio B. Magtibay¹¹⁶, Kris Catangatang¹¹⁷, Ruby Sibulo¹¹⁷, Felipe Campos Yauce¹¹⁵, Dariusz Wasyl¹¹⁸, Celia Manaia¹¹⁹, Jaqueline Rocha¹¹⁹, Jose Martins¹²⁰, Pedro Álvaro¹²⁰, Doris Di Yoong Wen¹²¹, Hanseob Shin¹²¹, Hor-Gil Hur¹²¹, Sukhwan Yoon¹²², Golubinka Bosevska¹²³, Mihail Kochubovski¹²³, Radu Cojocaru¹²⁴, Olga Burduniuc¹²⁵, Pei-Ying Hong¹²⁶, Meghan Rose Perry¹²⁷, Amy Gassama¹²⁸, Vladimir Radosavljevic¹²⁹, Moon Y. F. Tay¹³⁰,

Rogelio Zuniga-Montanez¹³⁰, Stefan Wuertz¹³⁰, Dagmar Gavačová¹³¹, Katarína Pastuchová¹³¹, Peter Truska¹³¹, Marija Trkov¹³², Karen Keddy¹³³, Kerneels Esterhuysen¹³⁴, Min Joon Song¹³⁵, Marcos Quintela-Baluja¹³⁶, Mariano Gomez Lopez¹³⁷, Marta Cerdà-Cuellar¹³⁸, R. R. D. P. Perera¹³⁹, N. K. B. K. R. G. W. Bandara¹³⁹, H. I. Premasiri¹³⁹, Sujatha Pathirage¹⁴⁰, Kareem Charlemagne¹⁴¹, Carolin Rutgersson¹⁴², Leif Norrgren¹⁴³, Stefan Örn¹⁴³, Renate Boss¹⁴⁴, Tanja Van der Heijden¹⁴⁵, Yu-Ping Hong¹⁴⁶, Happiness Houka Kumburu¹⁴⁷, Robinson Hammerthon Mdegela¹⁴⁸, Yaovi Mahuton Gildas Hounmanou⁹, Kaknokrat Chonsin¹⁴⁹, Orasa Suthienkul¹⁵⁰, Visanu Thamlikitkul¹⁵¹, Ana Maria de Roda Husman¹⁵², Bawimodom Bidjada¹⁵³, Berthe-Marie Njanpop-Lafourcade¹⁵⁴, Somtinda Christelle Nikiema-Pessinaba¹⁵⁵, Belkis Levent¹⁵⁶, Cemil Kurekci¹⁵⁷, Francis Ejobi¹⁵⁸, John Bosco Kalule¹⁵⁸, Jens Thomsen¹⁵⁹, Ouidiane Obaidi¹⁶⁰, Laila Mohamed Jassim¹⁶¹, Andrew Moore¹⁶², Anne Leonard¹⁶³, David W. Graham¹⁶⁴, Joshua T. Bunce¹⁶⁴, Lihong Zhang¹⁶³, William H. Gaze¹⁶³, Brett Lefor¹⁶⁵, Drew Capone¹⁶⁶, Emanuele Sozzi¹⁶⁷, Joe Brown¹⁶⁶, John Scott Meschke¹⁶⁸, Mark D. Sobsey¹⁶⁷, Michael Davis¹⁶⁹, Nicola Koren Beck¹⁶⁸, Pardi Sukapanpatharam¹⁶⁸, Phuong Truong¹⁶⁸, Ronald Lilienthal¹⁷⁰, Sanghoon Kang¹⁷¹, Thomas E. Wittum¹⁷², Natalia Rigamonti¹⁷³, Patricia Baklayan¹⁷³, Chinh Dang Van¹⁷⁴, Doan Minh Nguyen Tran¹⁷⁴, Nguyen Do Phuc¹⁷⁴, Geoffrey Kwenda¹⁷⁵, Bram van Bunnik¹⁷⁶, Mark Woolhouse¹⁷⁶, Fanny Berglund¹⁷⁷ & D. G. Joakim Larsson¹⁷⁷

⁴Institute of Public Health, Tirana, Albania. ⁵Universidad de Buenos Aires, Buenos Aires, Argentina. ⁶Melbourne Water Corporation, Melbourne, Australia. ⁷Charles Darwin University, Darwin, Australia. ⁸University of Copenhagen, Frederiksberg C, Denmark. ⁹Charles Darwin University, Darwin Northern Territory, Australia. ¹⁰Canberra Hospital, Canberra, Australia. ¹¹ALS Water, Scoresby, Australia. ¹²Austrian Agency for Health and Food Safety (AGES), Vienna, Austria. ¹³University of Dhaka, Dhaka, Bangladesh. ¹⁴Environmental Protection Department, Bridgetown, St. Michael, Barbados. ¹⁵Laboratoire Hospitalier Universitaire de Bruxelles (LHUB-ULB), Brussels, Belgium. ¹⁶AQUAFIN NV, Aartselaar, Belgium. ¹⁷Polytechnic School of Abomey-Calavi, Abomey-Calavi, Benin. ¹⁸Universidad Católica Boliviana San Pablo, La Paz, Bolivia. ¹⁹Public Health Institute of the Republic of Srpska, Faculty of Medicine University of Banja Luka, Banja Luka, Bosnia and Herzegovina. ²⁰Public Health Institute of the Republic of Srpska, Banja Luka, Bosnia and Herzegovina. ²¹Botswana International University of Science and Technology, Palapye, Botswana. ²²Universidade Federal de Minas Gerais, Belo Horizonte, Brazil. ²³Oswaldo Cruz Institute, Rio de Janeiro, Brazil. ²⁴Vale Institute of Technology, Belim, PA, Brazil. ²⁵National Center of Infectious and Parasitic Diseases, Sofia, Bulgaria. ²⁶University of Ouagadougou, Ouagadougou, Burkina Faso. ²⁷Institut Pasteur du Cambodge, Phnom Penh, Cambodia. ²⁸Centre Pasteur du Cameroun, Yaoundi, Cameroon. ²⁹University of Regina, Regina, Canada. ³⁰Eau Terre Environnement Research Centre (INRS-ETE), Quebec City G1K 9A9, Canada and Indian Institute of Technology, Jammu, India. ³¹Eau Terre Environnement Research Centre (INRS-ETE), Quebec City G1K 9A9, Canada and Lassonde School of Engineering, York University, Toronto, Canada. ³²University of N'Djamena, N'Djamena, Chad. ³³Escuela de Medicina Veterinaria, Facultad de Ciencias de la Vida, Universidad Andres Bello, Santiago, Chile. ³⁴Institute of Public Health, Santiago, Chile. ³⁵Universidad Católica del Maule, Centro de Biotecnología de los Recursos Naturales, Facultad de Ciencias Agrarias y Forestales, Talca, Chile. ³⁶Guangdong Provincial Center for Disease Control and Prevention, Guangzhou, China. ³⁷The Hong Kong Polytechnic University, Hong Kong, China. ³⁸Shantou University Medical College, Shantou, China. ³⁹Nanjing University of Information Science and Technology, Nanjing, China. ⁴⁰Center for Disease Control and Prevention of Henan province, Zhengzhou, China. ⁴¹Colombian Integrated Program for Antimicrobial Resistance Surveillance - Coipars, CI Tibaitatá, Corporación Colombiana de Investigación Agropecuaria (AGROSAVIA), Tibaitatá - Mosquera, Cundinamarca, Colombia. ⁴²Institut Pasteur de Côte d'Ivoire, Abidjan, Côte d'Ivoire. ⁴³University of Zagreb, Zagreb, Croatia. ⁴⁴Andrija Stampar Teaching Institute of Public Health, Zagreb, Croatia. ⁴⁵Veterinary Research Institute, Brno, Czech Republic. ⁴⁶Centre de Recherche en Sciences Naturelles de Lwiro (CRSN-LWIRO), Bukavu, Democratic Republic of Congo. ⁴⁷BIOFOS A/S, Copenhagen K, Denmark. ⁴⁸Technical University of Denmark, Kgs, Lyngby, Denmark. ⁴⁹Suez Canal University, Ismailia, Egypt. ⁵⁰University of Sadat City, Sadat City, Egypt. ⁵¹Ministry of Health, Environmental Microbiology, Tallinn, Estonia. ⁵²Addis Ababa University, Addis Ababa, Ethiopia. ⁵³University of Helsinki, Helsinki, Finland. ⁵⁴French Institute Search Pour L'exploitation De La Mer (Ifremer), Nantes, France. ⁵⁵Instituto Nacional de Investigación en Salud Pública-INSPI (CRNRAM), Galapagos, Quito, Ecuador. ⁵⁶National Public Health Laboratories, Ministry of Health and Social Welfare, Kotu, Gambia. ⁵⁷National Center for Disease Control and Public Health, Tbilisi, Georgia. ⁵⁸Robert Koch Institute, Berlin, Germany. ⁵⁹Technische Universität Dresden, Institute of Hydrobiology, Dresden, Germany. ⁶⁰University for Development Studies, Tamale, Ghana. ⁶¹University of Ghana, Accra, Ghana. ⁶²Kwame Nkrumah University of Science and Technology, Kumasi, PMB, Ghana. ⁶³Council for Scientific and Industrial Research Water Research Institute, Accra, Ghana. ⁶⁴Veterinary Research Institute of Thessaloniki, Hellenic Agricultural Organisation- DEMETER, Thessaloniki, Greece. ⁶⁵Athens Water Supply and Sewerage Company (EYDAP S.A.), Athens, Greece. ⁶⁶Universidad de San Carlos de Guatemala, Guatemala City, Guatemala. ⁶⁷Semmelweis University, Institute of Medical Microbiology, Budapest, Hungary. ⁶⁸University of Veterinary Medicine, Budapest, Hungary. ⁶⁹University of Iceland, Reykjavik, Iceland. ⁷⁰Cochin University of Science and Technology, Cochin, India. ⁷¹Kasturba Medical College, Manipal, India. ⁷²Apollo Diagnostics, Mangalore, India. ⁷³Shiraz University of Medical Sciences, Shiraz, Iran. ⁷⁴Shahid Beheshti University of Medical Sciences, Tehran, Iran. ⁷⁵National University of Ireland Galway, Galway, Ireland. ⁷⁶Ben Gurion University of the Negev and Ministry of Health, Beer-Sheva, Israel. ⁷⁷Istituto Zooprofilattico Sperimentale del Lazio e della Toscana, Rome, Italy. ⁷⁸CNR - Water Research Institute, Verbania, Italy. ⁷⁹National Institute of Infectious Diseases, Tokyo, Japan. ⁸⁰National Center of Expertise, Taldykorgan, Kazakhstan. ⁸¹Mount Kenya University, Thika, Kenya. ⁸²Kenya Medical Research Institute, Nairobi, Kenya. ⁸³University of Prishtina "Hasan Prishtina" & National Institute of Public Health of Kosovo, Prishtina, Kosovo. ⁸⁴Kuwait Institute for Scientific Research, Kuwait City, Kuwait. ⁸⁵Institute of Food Safety, Riga, Latvia. ⁸⁶American University of Beirut, Beirut, Lebanon. ⁸⁷Central Michigan University & Michigan Health Clinics, Saginaw, MI, USA. ⁸⁸National Food and Veterinary Risk Assessment Institute, Vilnius, Lithuania. ⁸⁹Luxembourg Institute of Science and Technology, Belvaux, Luxembourg. ⁹⁰Institut Pasteur de Madagascar, Antananarivo, Madagascar. ⁹¹University of Antananarivo, Centre d'Infectiologie Charles Mirieux, Antananarivo, Madagascar. ⁹²University of Malawi, Blantyre, Malawi. ⁹³Malaysian Genomics Resource Centre Berhad, Kuala Lumpur, Malaysia. ⁹⁴AIMST University, COMBio, Kedah, Malaysia. ⁹⁵Water Services Corporation, Luqa, Malta. ⁹⁶Environmental Health Directorate, St. Venera, Malta. ⁹⁷University of Mauritius, Reduit, Mauritius. ⁹⁸Institute for Public Health Montenegro, Podgorica, Montenegro. ⁹⁹Institut Pasteur du Maroc, Casablanca, Morocco. ¹⁰⁰Centro de Investigación em Saúde de Manhiça (CISM), Maputo, Mozambique. ¹⁰¹Agriculture and Forestry University, Kathmandu, Nepal. ¹⁰²National Institute for Public Health and the Environment (RIVM), Bilthoven, The Netherlands. ¹⁰³University of Otago, Dunedin, New Zealand. ¹⁰⁴University of Otago, Christchurch, New Zealand. ¹⁰⁵University of Central America, Managua, Nicaragua. ¹⁰⁶Universidad Nacional Autónoma de Nicaragua-León, León, Nicaragua. ¹⁰⁷University of Ilorin, Ilorin, Nigeria. ¹⁰⁸University of Ibadan, Ibadan, Nigeria. ¹⁰⁹Norwegian Institute of Public Health, Oslo, Norway. ¹¹⁰VEAS, Slemmestad, Norway. ¹¹¹University of Agriculture, Faisalabad, Pakistan. ¹¹²Aga Khan University, Karachi, Pakistan. ¹¹³Laboratorio Central de Salud Pública, Asuncion, Paraguay. ¹¹⁴Instituto

Nacional de Salud, Lima, Peru. ¹¹⁵Universidad de Piura, Piura, Peru. ¹¹⁶WHO Environmental and Occupational Health, Manila, Philippines. ¹¹⁷Maynilad Water Services, Inc, Quezon City, Philippines. ¹¹⁸National Veterinary Research Institute, Pulawy, Poland. ¹¹⁹Universidade Católica Portuguesa, CBQF - Centro de Biotecnologia e Química Fina - Laboratório Associado, Escola Superior de Biotecnologia, Porto, Portugal. ¹²⁰Aguas do Tejo Atlântico, Lisboa, Portugal. ¹²¹Gwangju Institute of Science and Technology, Gwangju, Republic of Korea. ¹²²Korea Advanced Institute of Science and Technology, Daejeon, Republic of Korea. ¹²³Institute of Public Health of the Republic of North Macedonia, Skopje, Republic of North Macedonia. ¹²⁴State Medical and Pharmaceutical University, Chişinău, Republic of Moldova. ¹²⁵National Agency for Public Health, Chişinău, Republic of Moldova. ¹²⁶King Abdullah University of Science and Technology, Thuwal, Saudi Arabia. ¹²⁷University of Edinburgh, Edinburgh, Scotland, UK. ¹²⁸Institut Pasteur de Dakar, Dakar, Senegal. ¹²⁹Institute of Veterinary Medicine of Serbia, Belgrade, Serbia. ¹³⁰Nanyang Technological University, Singapore, Singapore. ¹³¹Public Health Authority of the Slovak Republic, Bratislava, Slovakia. ¹³²National Laboratory of Health, Environment and Food, Ljubljana, Slovenia. ¹³³Independent consultant, Johannesburg, South Africa. ¹³⁴Daspoort Waste Water Treatment Works, Pretoria, South Africa. ¹³⁵Korea Advanced Institute of Science and Technology, Daejeon, South Korea. ¹³⁶School of Veterinary Sciences, Lugo, Spain. ¹³⁷Labaqua, Santiago de Compostela, Spain. ¹³⁸IRTA, Centre de Recerca en Sanitat Animal (CRESA, IRTA-UAB), Campus de la Universitat Autònoma de Barcelona, Bellaterra, Spain. ¹³⁹University of Kelaniya, Ragama, Sri Lanka. ¹⁴⁰Medical Research Institute, Colombo, Sri Lanka. ¹⁴¹Caribbean Public Health Agency, Castries, Saint Lucia. ¹⁴²The Sahlgrenska Academy at the University of Gothenburg, Gothenburg, Sweden. ¹⁴³Swedish University of Agricultural Sciences, Uppsala, Sweden. ¹⁴⁴Federal Food Safety and Veterinary Office (FSVO), Bern, Switzerland. ¹⁴⁵Ara Region Bern AG, Herrenschwanden, Switzerland. ¹⁴⁶Centers for Disease Control, Taipei, Taiwan. ¹⁴⁷Kilimanjaro Clinical Research Institute, Moshi, Tanzania. ¹⁴⁸Sokoine University of Agriculture, Morogoro, Tanzania. ¹⁴⁹Faculty of Science and Technology, Suratthani Rajabhat University, Surat Thani, Thailand. ¹⁵⁰Faculty of Public Health, Mahidol University, Bangkok, Thailand. ¹⁵¹Faculty of Medicine Siriraj Hospital, Bangkok, Thailand. ¹⁵²National Institute for Public Health and the Environment (RIVM), Bilthoven, Netherlands. ¹⁵³National Institute of Hygiene, Lomé, Togo. ¹⁵⁴Agence de Médecine Préventive, Dapaong, Togo. ¹⁵⁵Division of Integrated Surveillance of Health Emergencies and Response, Lomé, Togo. ¹⁵⁶Public Health Institution of Turkey, Ankara, Turkey. ¹⁵⁷Hatay Mustafa Kemal University, Hatay, Turkey. ¹⁵⁸Makerere University, Kampala, Uganda. ¹⁵⁹Abu Dhabi Public Health Center, Abu Dhabi, United Arab Emirates. ¹⁶⁰Dubai Municipality, WWTP Al Aweer, Dubai, UAE. ¹⁶¹Rashid Hospital, Dubai, UAE. ¹⁶²Northumbrian Water, Northumbria House, Abbey Road, Pity Me, Durham, UK. ¹⁶³University of Exeter Medical School, Cornwall, UK. ¹⁶⁴Newcastle University, Newcastle upon Tyne, UK. ¹⁶⁵Brightwater Treatment Plant, Woodinville, WA, USA. ¹⁶⁶Department of Environmental Sciences and Engineering, University of North Carolina at Chapel Hill, Chapel Hill, NC, USA. ¹⁶⁷University of North Carolina, Chapel Hill, USA. ¹⁶⁸University of Washington, Seattle, WA, USA. ¹⁶⁹Baylor University, Waco, USA. ¹⁷⁰Columbia Boulevard WWTP, Portland, USA. ¹⁷¹Eastern Illinois University, Charleston, USA. ¹⁷²The Ohio State University, Columbus Ohio, USA. ¹⁷³Laboratorio Tecnológico del Uruguay, Montevideo, Uruguay. ¹⁷⁴Institute of Public Health in Ho Chi Minh City, Ho Chi Minh, Vietnam. ¹⁷⁵University of Zambia, Lusaka, Zambia. ¹⁷⁶Centre for Immunity, Infection and Evolution, University of Edinburgh, Edinburgh, UK. ¹⁷⁷Centre for Antibiotic Resistance Research (CARE), University of Gothenburg, Gothenburg, Sweden.